Author:
Ahmad Fauzi, N. A.

Title:
In-vitro Investigation of Nitrogen-doped Titanium Dioxide as an Antimicrobial Filler in Polymeric Bonding Agents

IN-VITRO INVESTIGATION OF NITROGEN-DOPED TITANIUM DIOXIDE AS AN ANTIMICROBIAL FILLER IN POLYMERIC BONDING AGENTS

Nurul Aliaa Ahmad Fauzi
BDS (London), MFDS RCSEd, DDS in Orthodontics (Bristol), MOrth RCSEng

A dissertation submitted to the University of Bristol in accordance with the requirements for award of the degree of Doctor of Dental Surgery in Orthodontics in the School of Oral and Dental Sciences, Faculty of Medicine and Dentistry

September 2020

Word Count: 19,293

ABSTRACT

Aim: To develop a novel aesthetic resin composite using a nitrogen-doped titanium dioxide (N-TiO_2) filler that possesses photocatalytic antimicrobial properties against cariogenic bacteria.

Setting: Biomaterials and oral microbiology laboratories, Bristol Dental School.

Design: *In-vitro* study to produce an aesthetic composite resin, with long-term antimicrobial properties under visible light. This was done by incorporating a N-TiO_2 filler within the resin.

Methods: N-TiO_2 powder was manufactured by heating commercial TiO_2 with urea. Free radical release from the N-TiO_2 powder under visible light irradiation was analysed using spectrophotometry. The N-TiO_2 powder was incorporated into dental resin and the photocatalytic activity assessed using a dye under both visible light and dark conditions. Using XTT assay to measure the cellular metabolic activity, the antibacterial properties of the N-TiO_2 within the resin discs were tested against cariogenic bacteria.

Results: Doping nitrogen into TiO_2 resulted in a band gap shift towards the visible light spectrum, which enabled the compound to release reactive oxygen species when exposed to visible light. When incorporated into dental resin, the N-TiO_2 still demonstrated sustained release of reactive oxygen species, maintaining its photocatalytic activity and showing an antibacterial effect towards *Streptococcus mutans* under visible light conditions.

Conclusions: N-TiO_2 filled resin showed great promise as a potential aesthetic resin-based adhesive for orthodontic bonding.

DEDICATION AND ACKNOWLEDGEMENTS

I would like to express my very great appreciation to my supervisors, Professor Tony Ireland, Professor Bo Su, and Dr Nihal Bandara, for providing guidance and feedback throughout this project. I am truly grateful for the continuous encouragement and support given.

A special thanks to my lab colleagues, for their assistance which allowed me to complete the laboratory stages of the research.

Finally, I am extremely grateful for my family. Thank you from the bottom of my heart for all the strength, love, and prayers you have given me. I could not have made it this far without you.

AUTHOR'S DECLARATION

I declare that the work in this dissertation carried put in accordance with the requirements of the University's Regulations and Code of Practice for Research Degree Programmes and that it has not been submitted for any other academic award. Except where indicated by specific reference in the text, the work is the candidate's own work. Work done in collaboration with, or with the assistance of others is indicated as such. I have identified all material in this dissertation which is not my own work through appropriate referencing and acknowledgement. Where I gave quoted or otherwise incorporated material which is the work of others, I have included the source in the references. Any views expressed in the dissertation, other than referenced material, are those of the author.

Signed: Nurul Aliaa Ahmad Fauzi Date: 01/07/2020

TABLE OF CONTENTS PAGE

LIST OF TABLES PAGE

LIST OF FIGURES PAGE

1. INTRODUCTION

The main reason why patients seek orthodontic treatment is to improve their dental aesthetics, and it seems the demand for such treatment continues to increase (Bayat *et al.,* 2017). Recent advances in technology continue to fuel this demand, with orthodontic appliances such as clear aligners, lingual fixed appliances and aesthetic labial appliances becoming much more acceptable, particularly for adult patients. These are less noticeable than conventional metal labial appliances and in some cases are virtually invisible. Despite these advances, labial fixed appliances, be it tooth-coloured or metal, are still the mainstay orthodontic appliances, and are commonly bonded to the teeth using resin-based adhesives. An unwanted side-effect of labial fixed appliances is the formation of white spot lesions (WSL) on the enamel surface, and every effort should be made to prevent their formation. Unfortunately, most preventative approaches currently available require a degree of patient compliance to be successful and a non-compliance approach is likely to be more successful.

This review will focus on evaluating the current evidence on white spot lesions, the non-compliance methods available to reduce their formation, a brief summary on bracket materials, dental adhesives, nanotechnology in dentistry and orthodontics, and finally the properties and the current use of titanium dioxide as a potential antimicrobial agent against cariogenic bacteria.

2. REVIEW OF THE LITERATURE

2.1. White Spot Lesions

White spot lesions (WSL) are defined as subsurface enamel porosities that arise as a result of early carious demineralisation (Summitt *et al.*, 2006). Their formation is a significant and unwanted side effect of orthodontic treatment. WSL can present as early as four weeks following the placement of orthodontic brackets. The most common teeth to be affected are the maxillary lateral incisors, mandibular canines and mandibular second premolars (Geiger *et al.*, 1992). They are most frequently found on the labial surfaces of the teeth, around the brackets, near the gingival margins and middle third of the labial surface of the teeth, and beneath the archwire (Mattousch *et al.*, 2007). The true frequency of WSLs is unknown, with reports varying greatly from 2% to 96% (Chang *et al.*, 1997). This could be due to the different methods used to detect WSLs, which include visual inspection, photography, light-induced fluorescence, and fibre-optic trans illumination. The more sensitive quantitative laser technique will yield a higher prevalence rate of WSLs compared to visual inspection.

An early study to determine the prevalence of white spot formation after banding and bonding reported that 50% of patients undergoing orthodontic treatment would have one or more WSL (Gorelick *et al.*, 1982). This high figure should be of concern for patients, parents and clinicians, as subsequent research has shown that five years after completion of orthodontic treatment lesions may still be visible, with a higher incidence of WSL in affected patients when compared to untreated controls (Ogaard *et al.*, 1997). This would suggest that once WSLs form, they can be challenging to treat. Based on the results of these studies, WSLs are a side effect that the majority, if not all patients, undergoing orthodontic

treatment will experience. It is therefore important to focus on effective prevention of this unwanted iatrogenic effect of orthodontic treatment.

2.2. Formation of WSLs

Once an orthodontic appliance has been fitted, there is a rapid shift in bacterial flora in the dental plaque, with research showing that the level of *Streptococcus mutans* (*S. mutans*) is significantly increased (Glans *et al.*, 2003). This increase in the level of cariogenic bacteria lowers the resting pH of plaque, such that fermentable carbohydrates found in the dental biofilm act as a nutrient source for these bacteria, with acids produced as a by-product. These acids will demineralise the hydroxyapatite within the enamel, leading to a change in the porosity, mineral content and surface shine. These changes will directly affect the refractive index of the tooth surface, leading to the visual opacity that is seen as a white patch (Gorelick *et al.*, 1982).

2.3. Factors associated with WSLs in orthodontic patients

The components of the orthodontic fixed appliance act as plaque retentive surfaces, making mechanical removal of plaque by patients difficult. During appliance placement, it is crucial that the operator removes any excess adhesive around the bracket base periphery at the time of initial bond up, in order to remove stagnation areas. This is not always easy to achieve, but is important since scanning electron microscopy has shown that mature plaque biofilm is present on the composite adhesive adjacent to the orthodontic bracket base as early as 2-3 weeks after bonding (Sukontapatipark *et al.*, 2001). Excess composite is therefore an important predisposing factor to plaque accumulation. Due to the difference in coefficient of thermal expansion between the tooth and composite (Asmussen, 1985), and

the polymerisation micro shrinkage of the composite resin upon curing (Lee *et al.*, 1986), a 10 μm gap width between the composite-enamel junction at the base of the bracket is sometimes formed. This gap can act as a zone of plaque accumulation. In addition to these factors, patients requiring orthodontic treatment, by their very nature, are the ones most likely to have malpositioned teeth, which in combination with the fixed appliance, may make effective oral hygiene challenging to perform.

2.4. Patient dependent methods in the prevention of WSLs

Before commencing orthodontic treatment, it is vital that patients understand the associated risks and how they might reduce them. Prevention begins by implementing a good oral hygiene regimen through correct tooth brushing and the use of a fluoridated toothpaste. Orthodontic patients are regularly reviewed every six weeks, allowing clinicians to monitor the standard of their oral hygiene. Periodic reinforcement is often required in order to re-motivate patients with poor compliance. In addition, it is recommended that a daily fluoride mouth rinse (0.05% NaF^-) is used (Marinho *et al.*, 2016), and at a different time to tooth brushing. The exposure of enamel to fluoride during orthodontic treatment reduces decalcification (van der Linden and Dermaut, 1998), but relies heavily on patient compliance. The patients that are most at risk of getting WSLs are also those least likely to adhere to additional preventative methods.

2.5. Non-compliance methods to prevent WSLs

Alternative non-compliance methods to prevent the formation of WSLs have been investigated and will be covered in the following sections.

2.5.1. Fluoride

Dental caries is the net result of consecutive cycles of de- and remineralisation of the dental hard tissues, and is a dynamic process involving the flow of calcium and phosphate to and from the enamel (Fejerskov and Kidd, 2008). Fluoride is thought to have a preventative effect on WSL through its effect on this demineralisation and remineralisation process.

The mineral component of enamel comprises mainly calcium-deficient carbonate hydroxyapatite, which is more soluble than pure calcium hydroxyapatite (LeGeros and Tung, 1983; Featherstone *et al.*, 1990; Kautsky and Featherstone, 1993). Fluoride is thought to reduce the amount of this more soluble, mainly calcium-deficient carbonate hydroxyapatite, through ionic exchange, with fluoride ions replacing the hydroxyl ions and creating a more stable fluoroapatite structure. Complete substitution of the fluoride into the crystal structure produces fluoroapatite. However, it is thought only 10% of the available fluoride can be incorporated in the enamel surface in this way (Margolis and Moreno, 1990). Nevertheless, fluoride in concentrations as low as 1 part per million (ppm) can lessen or inhibit enamel demineralisation (Margolis and Moreno, 1990), by providing improved protection against acid dissolution of the enamel prisms.

When the environment surrounding the enamel falls below the critical pH of 5.5, as occurs in dental plaque, it results in the diffusion of calcium and phosphate ions out of the enamel surface and into the oral environment. As the pH returns above 5.5, re-adsorption of these ions back into the tooth surface can occur, allowing the damaged crystals to be repaired, and in a form that is even more resistant to further acid attack (ten Cate and Featherstone, 1996). The continued presence of fluoride in the solution or biofilm surrounding the

hydroxyapatite crystals at this time is important, as it enhances this remineralisation process. The fluoride will be adsorbed to the surface of the demineralised crystals and will attract the calcium and phosphate ions, which will then be incorporated into the remineralised surface.

Although fluoride has a direct effect on demineralisation/remineralisation as outlined, it may also have a possible indirect effect through its mode of action on the bacteria involved in dental caries. At a low pH, fluoride diffuses into the bacterial cell wall as weak hydrofluoric acid (HF). Once inside the cell, HF will dissociate into H^+ and F^- ions. The continued diffusion and dissociation of H^+ ions lead to the acidification of the cytoplasm, which will have a negative effect on enzyme activity. Furthermore, the accumulation of fluoride ions interferes with enolase enzyme activity, inhibiting the carbohydrate metabolism of the cariogenic bacteria (Rosin-Grget *et al.*, 2013).

There are two principal methods of fluoride delivery to orthodontic patients that can be utilised during a course of treatment (Benson *et al.*, 2005). The first is topical application *e.g*. a fluoride containing gel, mouth rinse, varnish, or toothpaste. A systematic review found moderate quality evidence that the application of fluoride varnish every six weeks can reduce the formation of WSLs by up to 70% (Benson *et al.*, 2013). However, varnishes can be easily abraded and removed by tooth brushing and oral function within just a few days of application (Demito *et al.*, 2004). The second method is through the use of fluoride releasing materials, such as elastic modules or adhesives, and will be discussed in a later section.

Due to a paucity of good quality trials, there are no firm recommendations as to the best method or combined methods of fluoride delivery during a course of orthodontic treatment. Given this, the daily use of a 0.05% fluoride mouth rinse and a fluoridated toothpaste are suggested until enough high-quality evidence becomes available to suggest otherwise (Marinho *et al.*, 2016).

2.5.2. Chlorhexidine (CHX) varnish

Chlorhexidine gluconate (CHX) is an antimicrobial that works by binding to negatively charged bacterial cell walls, altering the permeability and causing fluid to leak intracellularly. The stability of the osmotic balance of the cell wall is affected, which ultimately leads to lysis and cell death. CHX has been extensively studied for the past four decades, primarily in its ability to prevent gingivitis. It is bacteriostatic at low concentrations and bactericidal at higher concentrations (Puig Silla *et al.*, 2008).

CHX is a broad-spectrum antimicrobial and can effect Gram-positive and Gram-negative bacteria, fungi, and yeasts, which makes it a unique antiseptic for controlling microbial populations (Emilson, 1977; Marsh, 1993). However, the length of any effect will be modified intra-orally by the presence of saliva and the continuous movement of the oral membranes.

There are a number of methods available to deliver CHX intraorally including mouth rinses, gels, sprays, chewing gum, dentifrices and varnishes (Olympio *et al.*, 2006). CHX varnishes require a professional application and are therefore not reliant on patient compliance. In addition, it offers a method of application that is site specific.

The antimicrobial properties of CHX not only act on periodontal pathogens, but also cariogenic bacteria such as *S. mutans* and *S. sobrinus* (Jarvinen *et al.,* 1995). Several articles have been published on the efficacy of CHX varnish against *S. mutans*. Most studies concluded that CHX has a suppressive and inhibitory effect towards *S. mutans* (Epstein *et al.,* 1991*;* Sari and Birinci*,* 2007*;* Evans *et al.,* 2015*)*. It is expected that this inhibitory effect would prevent or at least reduce the formation of WSLs. However, a split-mouth trial found that even though the proportion of *S. mutans* was low in plaque following the application of CHX varnish, there was no significant difference in the incidence of WSLs around the brackets and gingival margins of patients with fixed appliances, when compared to a placebo (Twetman *et al.*, 1995).

A recent systematic review, evaluating 11 articles on the effectiveness of CHX varnish in patients with fixed appliances, found only weak evidence to suggest it is an effective antimicrobial agent against *S. mutans* when used at intervals of 3-4 weeks (Tang *et al.*, 2016). Furthermore, side effects such as staining, taste impairment and mucositis may affect patients' compliance and acceptance of its application (Matthijs and Adriaens, 2002).

2.5.3. Chlorhexidine-releasing glass ionomer cement (GIC)

The antimicrobial effect of incorporating chlorhexidine into GIC restorative materials and luting cement has also been investigated (Ribeiro and Ericson, 1991; Hoszek and Ericson, 2008). Studies showed that CHX has an inhibitory effect on *S. mutans,* which is dose dependent. The addition of 10% and 18% CHX to GIC, increased antimicrobial properties against *S. mutans* with the inhibition zone at the higher concentration being larger (Farret *et*

al., 2011). Despite this, it was not clear if the long-term effect of chlorhexidine would be maintained, as the experiment was done over a period of only 65 days.

2.5.4. Casein phosphopeptide-amorphous calcium phosphate (CPP-ACP)

The use of CPP-ACP nanocomplexes is a technology based on ACP stabilised by casein phosphopeptides (CPP) (Cross *et al.*, 2005). It is a milk based product that can be used to effectively deliver calcium and phosphate ions to the tooth surface, promoting enamel remineralisation and helping to prevent dental caries (Reynolds, 1998). As well as the CPP-ACP binding readily to the surface of the tooth, it can infiltrate the salivary pellicle and inhibit the adherence of *S. mutans*. An acidic environment is required to allow the ions to diffuse into the enamel subsurface. Therefore, under acidic conditions CPP-ACP localised to the tooth surface is able to release free calcium and phosphate ions into plaque, thereby providing a supersaturated environment that inhibits enamel demineralisation and promotes remineralisation.

CPP-ACP can be delivered via different methods, including chewing gum (Morgan *et al.,* 2008), mouth rinses (Reynolds *et al*., 2003), lozenges (Cai *et al*., 2003), and dentifrices.

The addition of 2% CPP-ACP to a 1100 ppm fluoride dentifrice increases enamel subsurface remineralisation by 156% relative to that produced by 1100 ppm fluoride alone. The use of fluoride toothpaste along with CPP-ACP containing dentifrice, has proved to be beneficial in reducing the white spot lesions around orthodontic brackets (Sudjalim *et al.,* 2007). Although this may seem promising, CPP-ACP containing dentifrice is expensive and for this reason is not widely available.

Xylitol chewing gum containing CPP-ACP has been found to produce a dose-related increase in enamel remineralisation (Shen *et al.*, 2001). Furthermore, a randomised, double-blind crossover *in-situ* study concluded that CPP-ACP containing chewing gum produces 107% greater remineralisation of enamel than sugar-free non-CPP-ACP containing gum (Manton *et al.*, 2008). Even though CPP-ACP can be found in commercial products, it is not suitable to be used as a filler in restorative materials due to insufficient and equivocal evidence supporting its clinical use (Braga *et al*., 2019).

The incorporation of ACP as bioactive filler in orthodontic bonding resin has also been tested as a means of delivering calcium and phosphate ions to the enamel surface around orthodontic brackets. After an acid challenge, the material has the potential to self-activate in a low pH environment by releasing calcium and phosphate ions, which are then deposited into the tooth structure as an apatite mineral, similar to the hydroxyapatite found in enamel (Uysal *et al.*, 2010). An *in-vivo* study comparing the micro hardness of the enamel around brackets bonded to teeth using either an ACP containing orthodontic adhesive or conventional composite resin adhesive found that the former reduces enamel decalcification in patients with poor oral hygiene (Uysal *et al.*, 2010). However, this was a short 30-day study with no data on the long-term release of the calcium and phosphate ions from the ACP containing adhesive. In addition, another study found the observed bond strength of the ACP containing adhesive to be significantly weaker than conventional resin adhesives (Foster *et al.*, 2008), which may be a potential limitation. Currently, there is insufficient clinical trial data to make a recommendation on the long-term effectiveness of CPP-ACP containing adhesives during orthodontic treatment.

2.5.5. Laser therapy

Irradiation of enamel with high power argon or CO_2 lasers can alter the surface morphology and composition of the enamel, making it more caries resistant. The calcium-phosphate ratio is modified, leading to the formation of more stable and less acid-soluble compounds. The CO_2 laser is able to control mineral loss of the enamel at the same level as those obtained with fluoride alone (Sadr Haghighi *et al.*, 2013). Furthermore, an *in-vivo* investigation on 65 human teeth used to study the effect of the CO_2 laser found that enamel demineralisation was prevented even after repeated acid challenges due to surface rehardening (Paulos *et al.,* 2017). However, there are some conflicting findings about the use of lasers for enamel surface modification (von Fraunhofer *et al.*, 1993; Ying *et al.*, 2004). SEM of treated enamel revealed that lased areas had melted, and the surface had been thermally degenerated. This raises the concern that high-energy laser irradiation may cause a temperature rise (above 1000^{o}C) that could have untoward thermal effects on the underlying dentine/pulp. This is to say nothing of the cost of the laser and the time required to use it.

2.5.6. Elastomeric ligatures containing antimicrobial agents

Elastomeric ligatures are changed frequently throughout a course of orthodontic treatment and as such have been considered as a means of antimicrobial delivery that does not rely on patient compliance. An *in-vivo* trial to investigate the effect of fluoridated elastomeric ligatures on the population of cariogenic bacteria, found that fluoride releasing elastomers were poor in controlling bacterial growth after a clinically relevant period of six weeks. In addition, the difference in mean mineral loss (vol %. µm) between enamel exposed to fluoridated elastomeric ligatures (477.2 SD 298.4) and non-fluoridated elastomers (599.3 SD

515.4) was considered to be both statistically and clinically insignificant (Doherty *et al.*, 2002). This could be due to the short-term nature of fluoride release, as another study reported that 88% of the active agent had leached out by the end of the second week of orthodontic treatment (Wiltshire, 1996).

Chlorhexidine (CHX) has also been used as the active agent within elastomeric materials (Jeon *et al.*, 2015), and although the rapid release of CHX was demonstrated for the first 24 hours in the case of all samples, there was no significant release after 48 hours. More recently, a laboratory study by Kamarudin (2017) found sustained CHX release of up to 57 days when the CHX was combined with hexametaphosphate in an elastomeric material.

Although there are commercially available stannous fluoride releasing elastomeric ligatures currently on the market (Fluor-I-Ties by Ortho Arch Company Inc), elastomeric containing active agents have not gained widespread acceptance, due not only to a lack of sustained release of active agents, but also due to changes in their physical properties when combined with antimicrobial agents (Wiltshire, 1996).

2.6. Orthodontic adhesives

Orthodontic adhesives are used to bond brackets, tubes and auxiliary attachments to the teeth. These adhesives should enable the brackets to stay bonded to teeth for the duration of treatment and allow easy debond when needed, and without causing damage to the enamel or discomfort to the patient (Rock and Abdullah, 1997; Klocke *et al.*, 2003). The introduction of new materials in recent years has blurred the line between materials

traditionally used for banding and those used for bonding. Currently available materials used as adhesives in orthodontics include:

- Diacrylates
- Glass polyphosphonate cement
- Glass polyalkenoate cement (GIC)
- Resin-modified glass ionomer cement (RMGIC)
- Polyacid-modified resin composites (Compomers)

2.6.1. Diacrylates

Buonocore first described the technique for dental bonding in 1955, but it was not until 1969 that this technique was used in combination with diacrylate resin to bond orthodontic attachments (Newman, 1969). Diacrylates consist of monomers, such as methyl methacrylate, which undergo free radical addition polymerisation on activation and initiation. The term composite is used when fillers are added to the resin, which usually comprises at least 50% by weight of the material (van Dijken, 1987). These filler particles alter the physical and thermal properties of the material by reducing the coefficient of thermal expansion, reducing polymerisation shrinkage and by increasing the abrasion resistance of the final product. These properties are useful if the composite is used as a filling material. However, the advantage if used in thin section underneath orthodontic brackets is questionable, although the use of fillers does improve the handling characteristics by improving the viscosity to the benefit of the orthodontist. The setting mechanisms if used as a bonding agent can either be chemical, light, or dual cured (Ireland and McDonald, 2003) (Table 1).

Setting Mechanism	Description
Chemical cured	**Twin Paste** • Activator and initiator in separate pastes. • Free radical reaction initiated as pastes are mixed. **No-mix** • Initiator painted by the operator on the tooth surface and bracket base. • Composite resin containing activator is applied to bracket base. • Rapid polymerisation takes place as bracket is pushed onto tooth surface.
Light cured	• Light sources (halogen, plasma arc, and LED) with wavelengths between 440-480nm activate the photo initiator, usually camphorquinone, in the composite resin to initiate free radical polymerisation.
Dual cured	• Can be cured chemically and with light exposure. • Less commonly used in orthodontics.

Table 1. The different setting mechanisms of diacrylates (Ireland and McDonald, 2003).

2.6.2. Cyanoacrylates

Researchers have long since been searching for an adhesive with a simplified bonding technique, capable of producing an effective bond with enamel that will last a course of orthodontic treatment, but that is also easy to debond at the completion of treatment. Cyanoacrylate, or super glue, is a single component adhesive, which can polymerise at room temperature without an additional catalyst, when in contact with only the smallest amount of moisture. This is known as anionic addition. Studies investigating the bond strength of cyanoacrylates in orthodontics found this adhesive not only to have poor performance compared with conventional diacrylic bonding agents, but that it was unstable after continuous exposure to moisture, making it unsuitable for clinical use (Howells and Jones, 1989; Crabb and Wilson, 1971; Al-Munajed *et al.*, 2000). A more recent clinical trial

confirmed this, with bond failure rates as high as 55.6% after just 12 months of treatment, compared with a failure rate of 11.3% for conventional composite resin (Le *et al.*, 2003).

2.6.3. Glass polyalkenoate cement (GIC)

Commonly known as glass ionomer cement (GIC), this adhesive was introduced by Wilson and Kent in 1972. There are two main components that make up this material. These are:

i. Organic acid in liquid form, such as polyacrylic acid and polymaleic acid.
ii. Ion leachable glasses in powder form, namely calcium aluminofluorosilicate.

When the powder and liquid are combined an acid-base reaction takes place. This can be described in four stages (Khoroushi and Keshani, 2013):

i. Dissolution stage
    - The acids interact with the surface of the glass particles to release metallic cations from the glass.
ii. Gelation stage
    - The Ca^{2+} cations bind to the carboxylate groups to form calcium polyacrylate chains, which begin to change the consistency of the mixture.
iii. Hardening
    - Progression of the reaction results in Al^{3+} ions becoming incorporated into the gel resulting in crosslinking of the polymer chains.
iv. Maturation
    - Much of the strength of the GIC is achieved after 24 hours. However, as the reaction continues, the bond strength increases due to continuous diffusion of the cations.

A well-known advantage of the cement is its fluoride releasing property, which increases soon after bonding or banding. Although fluoride release falls rapidly and is not maintained over time, decalcification rates beneath the brackets or bands have been reported to be lower when compared to zinc phosphate cement (Kvam *et al.*, 1983). However, this is not a universal finding, with more recent research comparing conventional GIC and zinc phosphate showing no statistically or clinically significant difference in the incidence of decalcification between the two cements when used for banding (Galarraga and Croce, 2003).

2.6.4. Glass polyphosphonate cement

This adhesive material uses a different acid component, namely polyacrylic acid. It sets more rapidly than conventional GIC (Ellis *et al.*, 1991; Clark *et al.*, 2003) and has a lower solubility and higher translucency. An *in-vivo* study found band failure rates to be comparable with conventional GIC, and when taste was investigated patients preferred the glass polyphosphonate cement, even though statistically there was no significant difference between it and the conventional GIC (Clark *et al.*, 2003). Despite this advantage, there is currently limited evidence to suggest that glass polyphosphonate cement reduces decalcification in the orthodontic patients.

2.6.5. Resin-modified glass polyalkenoate cement (RMGIC)

RMGIC is a hybrid material of conventional GIC with approximately 10% resin, namely HEMA (hydroxyethyl methacrylate) (Smith, 1998). As a result, it exhibits properties of both materials (Kumar and Kumari, 2016). When the powder and liquid are mixed, the cement sets by three reactions; acid-base, light cured polymerisation and chemical self-curing. The

acid-base reaction is similar to that of conventional GIC. Resin polymerisation is initiated on exposure to the light and the HEMA forms polyHEMA chains. This resin can also set by chemical polymerisation due to the intrinsic redox reaction and will auto-cure over time (Banerjee *et al.*, 2003). Clinical examples include Fuji II LC, Vitremer and Ketac Nano.

Advantages of RMGIC over conventional GIC include a long working time but rapid set by photocuring when required, and a more tolerant effect towards moisture due to the rapid development of early strength (Cook and Youngson, 1989; Chan *et al.*, 1990).

RMGIC has the potential to inhibit cariogenic bacteria due to its fluoride releasing properties similar to conventional GIC. However, a recent multicentre randomised clinical trial found that bonding with RMGIC did not reduce the incidence of demineralisation in patients who had fixed orthodontic appliances compared to those bonded with composite adhesive. Out of the 173 participants, only 42 were judged to have developed new WSLs after treatment, with occurrence higher in the RMGIC group by 21%. Even so when both groups were compared, the difference was not statistically significant (Benson *et al.,* 2019).

Additionally, an *in-vitro* study found no association between fluoride release from RMGIC and any long–term effect on bacterial viability (Fischman and Tinanoff, 1994). The peak antimicrobial activity against *S. mutans* occurred immediately after the material had set. However, with increasing time bacterial growth inhibition decreased. The authors suggested that a reduction in inhibition could be due to the increase in acid-tolerance of the microorganisms.

Similarly, in another study, the number of *S. mutans* colony-forming unit (CFU) was found to be smaller in plaque surrounding orthodontic brackets bonded with RMGIC than in plaque adjacent to brackets bonded with resin-based composite on the 15th day after placement of fixed appliance (Mota *et al.*, 2008). However, the inhibition effects of the RMGIC diminished over time, with increasing bacterial growth noted on days 30 and 45. The above studies suggest that antimicrobial activity only occurs in the initial phase and has no long-term cariostatic effect.

2.6.6. Polyacid-modified resin composites (Compomers)

Compomers are hybrid materials that provide the combined benefits of composites and glass ionomers. Unlike RMGIC, they do not bond to hard tooth-tissues, therefore should not be classified as glass ionomers. The primary setting reaction is by free radical addition polymerisation. Once the resin component has cured, water is absorbed into the material initiating the delayed acid-base reaction of the polyalkenoate glass particles. The flexural strengths are said to be better than RMGIC, but not as good as conventional resin adhesives (el-Kalla and Garcia-Godoy, 1999; Abu-Bakr *et al.*, 2000). In another study, it was reported that the survival rate of brackets bonded with compomer was comparable to resin adhesives (Millett *et al.*, 2000). Moreover, there was a statistically significant difference in decalcification of teeth at debond, with compomer (20%) producing less white spot lesions on labial surfaces of teeth compared to resin adhesive (26%). Despite this potential advantage, compomers have not gained widespread acceptance as orthodontic bonding or banding materials.

To date the evidence supporting the role of any one type of non-compliance method to reduce the incidence of WSL is limited.

2.7. Orthodontic brackets

Metallic brackets have been used most frequently in fixed orthodontic treatment, with the majority being stainless-steel of various grades (Maijer and Smith, 1982). The grey metallic colour makes this bracket material unpopular among adult patients. Apart from aesthetics, nickel contained in the brackets has the potential to elicit nickel allergy in some individuals (Rahilly and Price, 2003). The issue of nickel sensitivity has led to the introduction of alternative materials such as cobalt chromium and titanium as bracket materials. Cobalt chromium brackets contain about 0.5% nickel compared to 8-10% in stainless-steel brackets (Mihardjanti *et al.*, 2017). On the other hand, titanium brackets have 0% nickel, are biocompatible, non-allergenic and resistant to corrosion (Gioka *et al.*, 2004). Despite this, stainless steel is still the most frequently used metallic bracket material.

Plastic or polymeric brackets were introduced in the 1970s as an aesthetic alternative to metal brackets (Russell, 2005). Unfortunately, such brackets are really only suitable for very short courses of orthodontic treatment. This is primarily due to their low abrasion resistance and therefore increased wear, such that tie wings maybe lost relatively early on during treatment. However, they also demonstrate a low stiffness and a tendency to creep under continuous loading, both of which can lead to problems with a lack of torque transfer (Reynolds, 2016).

Another type of aesthetic bracket material is ceramic. This can exist in either the polycrystalline or monocrystalline form (Bishara and Fehr, 1997). Although ceramic orthodontic brackets have good aesthetic properties and do not distort under normal clinical loading, there have been issues with the strong bond seen at the bracket-adhesive interface, which increases the risk of damaging the tooth surface during the debonding process (Bishara *et al.,* 1994). This has led to bracket manufacturers altering the bonding base to reduce this risk.

2.8. Microbial profile of different bracket materials

An orthodontic fixed appliance, once fitted, encourages plaque accumulation, leading to increased *S. mutans* colonisation and subsequent decrease in pH in the tooth-plaque microenvironment, all of which can ultimately result in WSL and caries formation (Balenseifen and Madonia, 1970; Mizrahi, 1982). Bracket materials may play an important part in salivary pellicle formation and microbial attachment, but currently limited research has been done on the plaque retaining capacity of different types of brackets.

Salivary pellicle is a thin acellular film that is not limited to tooth surfaces. It can form on any surface including cementum, oral mucosal epithelium (Bradway *et al.*, 1989), dental restorations (Shahal *et al.*, 1998), implants (Edgerton *et al.*, 1996) and orthodontic attachments (Lee *et al.*, 2001). Proteins commonly found in salivary pellicle, including proline-rich proteins, α-amylase, MG1, and secretory IgA, are known receptors for bacterial adhesion (Hannig, 2002). The physical and chemical nature of the materials in the mouth such as the brackets, elastomers and adhesives will all affect the nature of salivary protein

adsorption, which in turn affects the binding affinity of selected microorganisms to the surface of the material.

There is conflicting evidence on the relationship between bracket materials and oral bacteria adhesion. For example, one study found that stainless steel, with its high surface energy, exhibited an increased potential for microbial adhesion, which in turn leads to an increased plaque retaining capacity when compared to polycarbonate and ceramic brackets (Eliades *et al.*, 1995). Conversely, others have reported plastic (Ahn *et al.*, 2007) or ceramic brackets (van Gastel *et al.*, 2009) exhibit greater bacterial adhesion. Meanwhile, Anhoury *et al.* (2002) concluded there was no significant difference in microbial profiles between different bracket types.

Overall, it is interesting to note the variability of outcomes from different studies. These experiments were mainly done *in-vitro* under simulated conditions, and with varying methodologies and therefore cannot be accurately extrapolated to an *in-vivo* setting. However, a knowledge of microbial profiles on different materials would allow us to fabricate appliances capable of interrupting the colonisation of cariogenic bacteria and hopefully reduce the incidence of WSL.

2.9. Nanotechnology

Nanotechnology is a branch of science which deals with particles less than 100nm in at least one dimension (Bhardwaj *et al.*, 2014) and was first described by Richard Feynman in 1959. It is a discipline which integrates many traditional subjects such as physics, chemistry, and materials science.

There are two main approaches to nanotechnology (Iqbal *et al.*, 2012). The 'Top-Down' approach, which involves fabrication of nanostructures by physically or chemically breaking down larger materials, for example through the process of milling, chemical vapour deposition or lithography. This approach has been used to produce various nanoscale coatings to improve functionality. An example would be the production of ultra-thin diamond-like coatings over vascular stents via chemical vapour deposition, in order to help improve biocompatibility and blood flow (Martinez and Chaikof, 2011).

Conversely, the 'Bottom-Up' approach creates material from the nanoscopic scale, atom-by-atom or molecule-by-molecule. Bottom-up processing is based on extremely organised chemical synthesis and growth of materials. It is more advantageous than the top-down approach because there is a better chance of producing nanostructures with fewer defects and with a more homogenous chemical composition.

At the nanoscale, materials may behave differently physically, chemically and biologically (Murph *et al.*, 2017). As a result, this can alter the bulk properties of a material, giving it for example, improved wear resistance or bactericidal properties. Perhaps not surprisingly, this has led to an interest in the potential application of nanoparticles in the fields of both medicine and dentistry (Mohamed Hamouda, 2012). Currently, nanomaterials are used widely for a range of medical applications, such as drug delivery, imaging to detect tumours and molecular diagnosis (Riehemann *et al.*, 2009). In dentistry, active research on nanomaterials has led to the production of various dental applications and these will now be described.

2.9.1. Nanotechnology in dentistry

The concept of nanotechnology in dentistry is not uncommon. Currently, several nanotechnology approaches are being applied. In restorative dentistry, the discovery of nanotechnology has led to the production of nanocomposites with less polymerisation shrinkage, higher strength and micro hardness and with improved aesthetics due to a better polishing ability (Bhardwaj *et al.*, 2014). An example of such a nanocomposite currently on the market is Filtek Supreme Universal by 3M^{TM}.

Calcium phosphate is another example of a nanoparticle which has self-healing and antimicrobial properties. This nanomaterial has been incorporated into a composite and the results were promising with reduced bulk fracture and reduced secondary caries formation (Wu *et al.*, 2015). However, the long-term antimicrobial effects were unclear.

In managing dentine hypersensitivity, the exposure of dentinal tubules can result in the movement of dentinal fluids due to thermal and osmotic factors. Using nanotechnology, carbonate-hydroxyapatite nanocrystals, which have the same structure as dentine, can be used to coat the exposed tubules and thereby reduce sensitivity (Matthias *et al.*, 2013).

Within endodontics, an effort has been made to produce an obturation material which has good thermal, mechanical and antimicrobial properties, by incorporating bioactive glass nanoparticles within the gutta percha mix. Root canal sealing was enhanced by the moisture expansion brought about by the bioactive glass nanoparticles within the gutta percha polymer (Mohn *et al.*, 2010).

2.9.2. Nanoparticles in orthodontics

In the manufacture of coatings on orthodontic archwires, nanoparticles have been used in an attempt to reduce the friction produced during orthodontic tooth movement. Fullerene-like nanoparticles, known for their lubricating properties, have been used to coat 0.019"x 0.025" stainless steel archwires, with the aim being to reduce friction between the archwire and bracket (Redlich *et al.*, 2008). The results of the laboratory tests showed a substantial reduction in the static friction at slot-wire angles of 0^{o}, 5^{o} and 10^{o}. However, the authors failed to mention whether there were any changes in the dimensions of the archwires following coating that might affect the degree of play of the archwires in the bracket slot. Exfoliation of the nanoparticles occurred as the load at the edges of the slot increased, and it was unclear if this might result in any toxicity or sensitivity issues as a result of potential exposure to the free nanoparticulate fullerene.

In order to harness any potential antimicrobial properties of nanoparticles in orthodontics, two approaches have been suggested (Borzabadi-Farahani *et al.*, 2014), namely:

- Incorporation of nanoparticles within the orthodontic adhesives
- Coating the surfaces of orthodontic appliances with nanoparticles

With the former approach, it is vital the physical and chemical properties of the nano-modified adhesives are not compromised. In one example, fluorapatite and hydroxyfluorapatite nanoparticles have been added to resin-modified glass ionomer cement to improve long-term fluoride release (Lin *et al.*, 2011). This study found that higher levels of fluoride were released throughout the experimental period of 70 days. However, this was

at the expense of a significant reduction in shear bond strength, which was considered to be at the lower limit of what might be acceptable for orthodontic bracket bonding.

Silver has long been recognised for its antimicrobial activity, indeed as early as 335 BC, during the rule of Alexander the Great, silver vessels were used to store and purify water (White, 2001). The addition of silver nanoparticles to composite adhesives has demonstrated improved antimicrobial properties, without compromising the observed bond strength of the cement. However, a limitation of such materials is their grey colouration, which would be a problem when used beneath aesthetic orthodontic brackets (Ahn *et al.*, 2009).

Antimicrobial activity has been tested on orthodontic brackets sputtered with N-TiO_2 using a magnetron (Cao *et al.*, 2013). When tested against microorganisms such as *S. mutans*, *Lactobacillus acidophilus*, *Actinomyces viscous* and *Candida albicans*, the results showed high antimicrobial activity and reduced bacterial adherence, particularly with *S. mutans*. Even though demineralisation and gingivitis can potentially be prevented, the problem with any antimicrobial coating, including of N-TiO_2, is that the coating will most likely be lost over time.

Nanoparticles incorporated into the bulk of a material are likely to show the greatest promise. However, it is vital both the physical and chemical properties (*e.g.,* bond strength, aesthetics, biocompatibility) of such a nano-modified material are not compromised, and that any antibacterial activity is maintained over time.

All of the above-mentioned studies have common limitations, namely that they have been carried out under laboratory conditions and lack long-term performance data.

2.9.3. Safety of nanotechnology

Nanotechnology has come a long way since it was first introduced and the potential for clinical applications appears real. However, various concerns have been raised regarding the uncertainty on the health hazards of nanomaterials. The potential for nanotechnology to improve clinical performance is basically due to the large surface area to volume ratio of such small materials. However, their small size also means they may potentially be absorbed through skin, lungs and digestive tract (Xia *et al.*, 2009). Accordingly, they have the potential to be retained in the body for years. Although currently there is no evidence of adverse toxicity reactions in humans, animal experiments have shown otherwise. In fact, a study on mice demonstrated that the inhalation of carbon nanotubes had a similar effect to the inhalation of asbestos (Poland *et al.*, 2008). Such particles are capable of activating pro-inflammatory effects that can lead to respiratory pathology. Moreover, nanoparticles can interact with the DNA, RNA and intercellular components altering their function and causing mutations (Singh *et al.*, 2013).

Various safety programs have been set up around the World to address the concerns regarding nanomaterials. In the UK, the Nanosafe Initiative was established with the mission of:

"…providing the highest quality expertise to help nanotechnology emerge and develop on a safe and sustainable basis, maximising its commercial potential, through a continuous

development and improvement of our knowledge, equipment and practice." (SafeNano, 2017).

Nanotechnology is a relatively new field. Therefore, there is a lack of long-term data on how it might harm human tissues and organs following long-term exposure. Insight on the potential threats and toxicity to humans can only be achieved by a fundamental change in approach from clinical trials in animals, to *in-vivo* testing on human beings.

2.10. Titanium dioxide (TiO_2)

The photocatalytic activity of TiO_2 under UV light has attracted increasing attention from researchers in various fields. TiO_2 is an example of a naturally occurring semiconductor and its light scattering property is utilised in industries and consumer products that require brightness and opacity (Zaleska, 2008). These include, but not limited to paints, plastics, rubber, cosmetics and even food and pharmaceutical supplements.

TiO_2 in the nanoparticle form is commonly used as a support material for photocatalytic applications such as the decontamination of harmful gas emissions (Peral *et al.*, 1997), disinfection of air and water (Crittenden *et al.*, 1997), self-cleansing glass or windows (Xu *et al.*, 2016) and biomedical applications (Rupp *et al.*, 2010).

Structurally, TiO_2 has three different crystal forms: rutile, anatase and brookite. Rutile and anatase are commonly used in photocatalysis, with higher photocatalytic activity being demonstrated by anatase. Although some studies have suggested that a mixture of rutile

and anatase is more photocatalytically active than pure anatase (Bacsa and Kiwi, 1998; Muggli and Ding, 2001a; Muggli and Ding, 2001b; Ohno *et al.*, 2001).

On exposure to UV light, TiO_2 will generate reactive oxygen species (ROS), which in turn leads to the decomposition of organic compounds. In this way, it demonstrates antibacterial properties towards a large number of bacteria, as well as being effective against fungi, algae, protozoa and mammalian viruses (Cai, 2013).

Ever since the discovery of UV light-induced water splitting by TiO_2 in 1972, a considerable number of studies have investigated the properties of TiO_2 (Fujishima and Honda, 1972). However, this photocatalytic property is not without its own set of challenges. Due to the wide band gap energy of TiO_2, this photocatalytic activation will only take place in the presence of UV light. The band gap is the energy required to promote an electron from the valence band to the conduction band when excited. The band gap for TiO_2 ranges from 3.0 eV to 3.2 eV depending on the composition of the crystal structure. This means that on exposure to UV light with an approximate wavelength of 385 nm, the photocatalytic property of TiO_2 can be activated. The electrons are then free to migrate, leaving a positively charged hole. These holes and free electrons are mobile. Two things can happen following this reaction. The positively charged holes and free electrons can recombine, thereby releasing heat, or they can migrate to the surface of the crystal where redox reactions can occur with various organic substances. This interaction with surface molecules will generate ROS, namely the hydroxyl radicals, hydrogen peroxide and superoxide radicals.

These photocatalytic properties of TiO_2 cannot be utilised effectively as UV light is needed to produce the ROS. UV radiation is widely recognised for its harmful effects on human skin which has led to the limited use of TiO_2 indoors or in dentistry applications. Therefore, in order to take the photocatalysis process toward sustainability, it is necessary to manufacture a material which can be activated by visible light. In order to achieve this, the band gap of TiO_2 has to be reduced. Less energy is needed to move the electron from the valence band to the conduction band. The lower energy required will correspond to the wavelength of the visible light (Figure 1). This has prompted researchers to investigate various ways in which the band gap might be shifted towards the visible part of the electromagnetic spectrum. A number of approaches have been suggested, and one of the most successful methods is the doping of non-metallic and metallic elements into the TiO_2 structure (Zaleska, 2008). These include metallic dopants such as Ag, Fe, V, Au and Pt, and non-metallic dopants such as N, S, C, B and P.

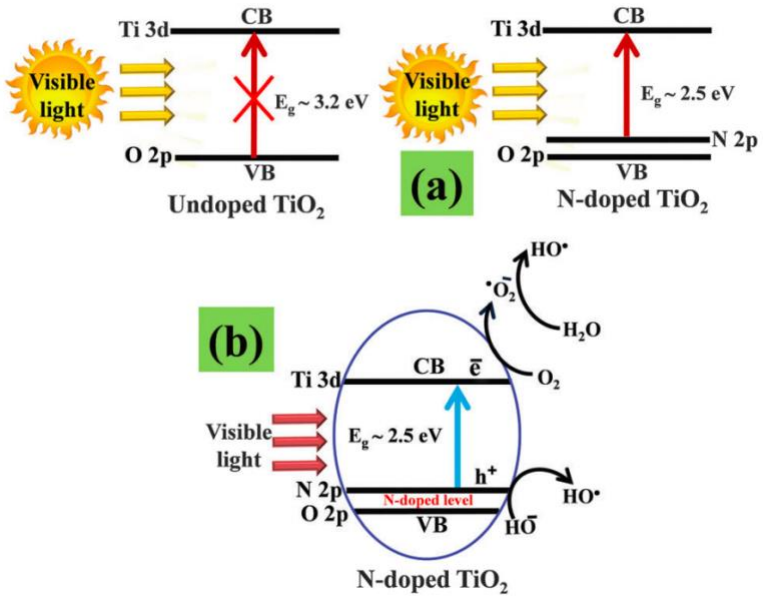

Figure 1. Diagram illustrating free radical release when light is applied to N-TiO2 compounds (Ansari *et al.*, 2016). Following nitrogen doping, there is reduction of intraband gaps created by the impurity, making it possible for visible light to excite the electrons residing in the valence band.

Recent research has shown that the antimicrobial properties of TiO_2 powder can be enhanced by doping silver (Ag) into the TiO_2 structure (Chambers *et al.*, 2017). The resulting powder was incorporated into a dental resin and the antimicrobial properties investigated. The study showed that Ag-TiO_2 nanoparticles incorporated within a resin composite were able to produce a significant bactericidal effect when in contact with *S. mutans* under visible light conditions. However, the resin discs changed from white to grey after being exposed to visible light and this was felt to be an issue if it was to be used as an orthodontic bonding adhesive, particularly with aesthetic brackets.

In addition, metal doping has been shown to have poor thermal stability, a low photocatalytic efficiency, has high recombinant rates and is costly as a result of the use of

noble and transition metals (Gosh and Das, 2015). This has led to non-metals being investigated as potential dopants.

Non-metal dopants, namely carbon and nitrogen, have been shown to improve the photocatalytic performance and morphology of TiO_2 (Daghrir *et al.*, 2013; Asahi *et al.,* 2014). Additionally, using nitrogen as dopant alters the hardness, elastic modulus, refractive index, and electrical conductivity of the TiO_2 (Lu *et al.*, 2007).

With these features in mind, the aim of the current study was to produce an antimicrobial nitrogen doped TiO_2 containing resin that could be used in orthodontics.

3. AIM AND OBJECTIVES

Aim

- To develop a novel aesthetic resin composite using nitrogen-doped titanium dioxide (N-TiO_2) filler that possesses antimicrobial properties against cariogenic bacteria.

Objectives

- To develop a TiO_2 filler powder that can be activated within the visible light spectrum through the incorporation of nitrogen (N).
- To determine the concentration of N within the TiO_2 powder that produces the maximum release of reactive oxygen species under visible light.
- To produce a resin composite that exhibits visible light photocatalytic properties by incorporation of N-TiO_2 powder.
- To investigate the aesthetic changes of resin composite containing a N-TiO_2 filler under different lighting conditions.
- To investigate the antimicrobial effects of resin containing a N-TiO_2 filler on cariogenic bacteria.

4. MATERIALS AND METHODS

Two sets of experiments will be described in the materials and methods. The first set involved just fabrication and testing of N-TiO_2 powders, and the second set involved the fabrication and testing of composite resin discs containing the different TiO_2 powders and at different wt%. The materials and numbers of specimens in each case are illustrated in Tables 2, 3, and 4.

4.1. Manufacture of N-TiO_2 powder

In order to produce N-TiO_2 powder with differing concentrations of N-doping, four different urea concentrations were used, namely 0.125, 0.25, 0.375, and 0.5 g. The powders were produced using the following materials and methods.

Materials and equipment

- 25 ml porcelain crucibles with lid, Fisher Scientific UK Ltd, Loughborough, UK
- Metal spatula, Fisher Scientific UK Ltd, Loughborough, UK
- Disposable weighing boats, Fisher Scientific UK Ltd, Loughborough, UK
- High temperature oven. Elite thermal system Ltd. Leicestershire, UK
- Urea powder, Sigma-Aldrich, Gillingham, Dorset, UK
- Titanium dioxide powder, Aeroxide™ P25, ACROS Organics™, Fisher Scientific UK Ltd Loughborough, UK
- Ethanol reagent, Sigma-Aldrich, Gillingham, Dorset, UK
- Agate pestle and mortar, Specac™, Fisher Scientific UK Ltd Loughborough, UK
- Sartorius weighing machine (TE 1502S) Sartorius Mechatronics UK Ltd, Surrey, UK
- 5mm diameter zirconia balls, Fisher Scientific UK Ltd, Loughborough, UK

- Speedmixer. DAC 150.1 FVZ-K. Synergy Devices Ltd, High Wycombe. Buckinghamshire, UK
- 100 ml polyethylene jar

Method

Firstly, 1.0 g of TiO_2 and 0.125 g of urea were separately measured using the Sartorius weighing scale and then manually ground using a pestle and mortar for 5 minutes. Following this, the mixture was transferred to a 100 ml polyethylene jar containing three 5 mm zirconia balls and was ground again, this time in a Speedmixer for 3 minutes at 2000 rpm, to produce a homogenous powder, before being transferred into a glass beaker containing 60 mL of ethanol. This was magnetically stirred at 150 rpm until complete evaporation of the solvent occurred, before being transferred to a porcelain crucible with a lid and calcined in an oven at 380^{o}C for 2 hours. Once cooled down to room temperature, the now pale-yellow sample was ground for a further 3 minutes at 2000 rpm using the Speedmixer. This was done as the powder tended to agglomerate following calcination. These steps were repeated with different urea loadings of 0.25, 0.375, and 0.5 g to produce four different concentrations of N-TiO_2 powders (Table 2).

4.2. Investigation of the band gap changes of N-TiO_2 powders

Materials and equipment

- Shimadzu UV-2600 UV-Vis Spectrophotometer, Shimadzu UK Limited, Milton Keynes, UK
- N-TiO_2 powders (0.125, 0.25, 0.375, and 0.5 g urea treated)
- Titanium dioxide powder, Aeroxide™ P25, ACROS Organics™, Fisher Scientific UK Ltd Loughborough, UK

- Sample cup and glass rod, Shimadzu UK Limited, Milton Keynes, UK

Method

The band gap shift of each of the four N-TiO_2 powders (Table 2) was assessed by compressing 0.5 g of each powder into a sample cup using a clean glass rod (Figure 2). The sample cup was then placed in the integrating sphere attachment located in the spectrophotometer with the lid closed. The reflectance from the UV-Vis spectrophotometer was measured on each sample three times, at wavelengths ranging from 200 to 500 nm. An average reading of each sample was plotted on a line graph. The band gap of each of the four N-TiO_2 powder was calculated using the Tauc plot method (Tauc, 1968).

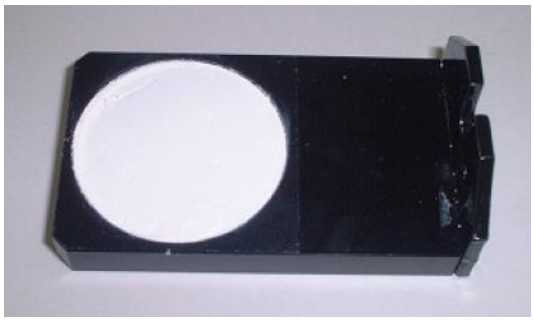

Figure 2. Pressed N-TiO_2 powder in a sample cup.

Figure 3. UV-Vis Spectrophotometer.

4.3. Investigation of the photocatalytic properties of undoped TiO_2 and N-TiO_2 powders under both light and dark conditions

The N-TiO_2 powders used in this experiment were again 0.125, 0.25, 0.375, and 0.5 g urea treated samples as described in section 4.1. Undoped TiO_2 powder was used as a control. The experiment in this section was repeated twice. The first was under visible light conditions and the second, under dark conditions. For each repeat, readings obtained from the spectrophotometer were done three times for each sample (See Table 2).

Material and equipment

- TiO_2 and N-TiO_2 powders (0.125, 0.25, 0.375, and 0.5 g urea treated)
- Shimadzu UV-2600 UV-Vis Spectrophotometer, Shimadzu UK Limited, Milton Keynes, UK
- Lux light meter, DVM1300, Velleman, Gavere, Belgium
- Rhodamine B dye, Sigma-Aldrich, Gillingham, Dorset, UK
- Desk lamp with a standard LED daylight light bulb, 6500K, 220-240V, Anglepoise laboratories, UK
- Magnetic stirring platform, Fisher Scientific UK Ltd, Loughborough, UK
- Disposable pipettes, Fisher Scientific UK Ltd, Loughborough, UK
- 50 ml beakers
- Deionsed water
- Measuring cylinder

Method

Rhodamine B dye solution with a concentration of 10 mg/L was prepared by dissolving 0.005 g of Rhodamine B powder into 500 ml of deionised water. 0.25 g samples of the 0.125, 0.25, 0.375, and 0.5 g of urea treated N-TiO_2 powders and undoped TiO_2 powder

were measured using the Sartorius weighing scale and added to separate glass beakers containing 50 ml of Rhodamine B dye. As a control, a separate beaker containing 50 ml of the Rhodamine B dye with no powder was prepared.

Prior to irradiation, each of the suspensions in the beakers were placed on a magnetic stirring platform and agitated gently with a flea magnet at 150 rpm for 30 minutes under dark conditions to facilitate the establishment of the adsorption-desorption equilibrium. This was achieved by covering the beakers with aluminium foil. A glass slab was used to cover the beakers to prevent evaporation of the solutions. After equilibration, the foils covering the beakers were removed and an adjustable desk lamp, used as the source of visible light, was positioned above the beakers at 2000 lux. The intensity of light was measured using a lux meter measured with a photodetector placed underneath the light source, at the same level as the Rhodamine B dye. The position of the lamp was adjusted relative to the Rhodamine dye level until the display on the meter reached 2000 lux.

While the solutions were exposed to the visible light, three samples of 3ml aliquots were withdrawn every 30 minutes, for 4 hours, from each beaker using a disposable pipette. Each collected solution was then dispensed in a plastic cuvette for absorption analysis on a UV-Vis spectrophotometer over a wavelength range of 200 to 500 nm. An average of the 3 readings was calculated for each solution and plotted on a line graph. Once the analysis by the spectrophotometer was completed, the solutions in the cuvette were transferred back to their respective beakers. The entire experiment was repeated again this time under dark conditions (Table 2).

Experiment	Urea (g)	Number of samples	Spectrophotometer readings/ sample	Repeats
4.1	0.125	1	-	-
	0.250	1	-	-
	0.375	1	-	-
	0.500	1	-	-
4.2	0.125	1	3	-
	0.250	1	3	-
	0.375	1	3	-
	0.500	1	3	-
4.3	0.125	1	3	2
	0.250	1	3	2
	0.375	1	3	2
	0.500	1	3	2

Table 2. The materials, number of samples, spectrophotometer readings and repeats (light and dark conditions) for each of the experiments 4.1, 4.2, and 4.3. In each case the initial powder contained 1 g of TiO_2.

4.4. Preparation of N-TiO_2 filled resin composite and colour assessment

In order to assess the effect of filler content on the colour of the resin discs, not only were the four different types of N-TiO_2 powders used, but the wt% loading of one of the powders within the resin (0.125 g urea treated) was also altered (Table 3).

Materials and equipment

- Disc-shaped silicone moulds
- 100 ml polyethylene jar
- N-TiO_2 powder (0.125, 0.25, 0.375, and 0.5 g urea treated)
- Disposable pipette, Fisher Scientific UK Ltd, Loughborough, UK
- Speedmixer. DAC 150.1 FVZ-K. Synergy Devices Ltd, High Wycombe. Buckinghamshire, UK
- Dental curing light, CU 100A, TPC Advanced Technology, California, USA
- Diurethane dimethacrylate (UDMA), Sigma-Aldrich, Gillingham, Dorset, UK
- Triethylene glycol dimethacrylate (TEGDMA), Sigma-Aldrich, Gillingham, Dorset, UK
- Ethyl 4-(dimethylamino) benzoate (4-EDMAB), Acros Organics, Fisher Scientific UK Ltd, Loughborough, UK
- Camphorquinone (CQ), Sigma-Aldrich, Gillingham, Dorset, UK
- Shade guide, VITA classical A1-D4, VITA Zahnfabrik, Germany
- Nikon DSLR Camera, 1/125s shutter speed, ISO 100, 100mm focal length, Nikon, D7200, Nikon Corporation, Japan

Method

In the preparation of the N-TiO_2 filled resin composite samples, a TEGDMA/UDMA resin mixture (50:50 wt/wt) containing the photoinitiator system CQ (0.2 wt%) and 4-EDMAB (0.8 wt%) was used. The measured TEGDMA was dispensed into a custom Speedmixer 100 ml polyethylene jar and heated in a water bath at 40^{o}C for 10 minutes. The photoinitiating system was added to the same polyethylene jar containing TEGDMA and spun using a Speedmixer for 5 minutes at 3000 rpm. UDMA was then added to the resin and photoinitiator system mixture and spun again for 3 minutes at 3000 rpm to ensure the

mixture was well dispersed. Finally, 1 wt% of 0.125 g of urea treated N-TiO_2 powder was added and mixed at 3000 rpm for 3 minutes in the Speedmixer.

Using a disposable pipette, the solution was then dispensed into silicone moulds to produce disc-shaped N-TiO_2 filled resin samples. The resin solution was irradiated using a dental curing light for 30 s to set the resin. The curing light was placed as close to the resin surface, but without touching it, while curing took place. Each disc had a diameter of 10 mm and a height of 1 mm. These steps above were repeated to manufacture resin discs containing 3, 5, 7, and 9 wt% of 0.125 g urea treated N-TiO_2 powder (Table 3). Increasing the powder content in the resin disc would increase the amount of N-TiO_2 exposed per unit surface area, therefore permitting more free radical release and higher photocatalytic activity.

To compare the effect of different initial urea loadings and therefore degrees of N-doping of the TiO_2 powders on the aesthetics of the resin discs, discs containing 0.25, 0.375, and 0.5 g of urea treated N-TiO_2 at 9 wt% were also manufactured using the same method as above (Table 3). The colour of each disc was compared visually with a shade guide immediately post-curing under natural sunlight. The shade that was observed closest in colour match to the shade guide was placed next to the disc over a black background and a photograph was taken using a digital camera. The colour assessment was repeated again 3 days later, by the same observer, under natural sunlight and recorded using the same method.

Experiment	N-TiO_2 filled resin disc (g of urea loading)	Number of Samples				
		1 wt%	3 wt%	5 wt%	7 wt%	9 wt%
4.4	0.125	1	1	1	1	1
	0.250	-	-	-	-	1
	0.375	-	-	-	-	1
	0.500	-	-	-	-	1

Table 3. The N-TiO_2 filled resin discs with different urea loadings and wt% as used in Experiment 4.4.

4.5. Preparation of N-TiO_2 filled resin discs with different surface treatments

In this part of the experiment, the effect of different resin disc surface treatments on free radical release, colour change under visible light, and antimicrobial activity were investigated.

Materials and equipment

- Tegrapol -15 polishing machine, Struers Ltd, Rotherham, UK
- Plasma Cleaner, Pico, Type A, Diener electronic GmbH + Co. KG, Germany

Method

0.125 g urea treated N-TiO_2 filled resin discs at 1,3,5,7, and 9 wt% were subjected to one of the following surface treatment methods listed below. These surface treatments were done to see if they would enhance the release of free radicals and photocatalytic activity as more N-TiO_2 powder should be exposed at the resin surface. The number of samples and the types of treatment the discs were exposed to are summarised in Table 4 and were also used in experiment 4.6.

A: No surface treatment (unpolished surface)

B: Plasma treatment only

C: Surface polish only

D: Surface polish and plasma treatment

Resin discs in the as-prepared condition were the unpolished samples. For the samples requiring plasma treatment, the discs were placed into a Diener Plasma Cleaner, powered to 200 W at 50 kPa for 30 minutes. In the case of the surface polished samples, they were polished using a Tegrapol -15 polishing machine with 1200 grit paper, for 15 seconds at 150 rpm. Samples subjected to both surface treatments were polished first using this same method before undergoing the plasma treatment.

4.6. Testing free radical release of N-TiO_2 filled resin composite at different nitrogen loadings with different surface treatments

Materials and equipment

- Measuring cylinder
- Deionised water
- 5ml beakers
- 20 ml glass vials
- 0.125 g urea treated N-TiO_2 filled resin discs (1, 3, 5, 7, 9 wt%)
- Disposable pipette, Fisher Scientific UK Ltd, Loughborough, UK
- Shimadzu UV-2600 UV-Vis Spectrophotometer, Shimadzu UK Limited, Milton Keynes, UK
- Rhodamine B dye, Sigma-Aldrich, Gillingham, Dorset, UK

Method

Rhodamine B dye solution with a concentration of 10 mg/L was prepared by dissolving 0.005 g of Rhodamine B powder in 500ml of deionised water. 10 ml of the dye solution was pipetted into four separate 20 ml glass vials.

Each sample containing 1 wt% of 0.125 g urea treated N-TiO_2 powder with surface treatments A, B, C and D was respectively added to four glass vials containing the dye solution. Prior to irradiation, the samples were left under dark conditions by covering the beakers with aluminium foil to establish adsorption-desorption equilibrium. After equilibration, the foils covering the beakers were removed and an adjustable desk lamp was positioned above the glass vials at an intensity of 2000 lux. The method used to measure the light intensity was as described in section 4.3.

A glass slab was used to cover the glass vials to prevent evaporation of the solutions. While the solutions were exposed to the visible light, three samples of 2 ml aliquots were withdrawn every 24 hours for 5 days from each glass vial using a disposable pipette and dispensed into a plastic cuvette for absorption analysis by a UV-Vis spectrophotometer over a wavelength range of 200 to 500 nm. Once the absorbance was measured, the solutions were then returned to their original glass vials. An average of the 3 readings was calculated for each solution and plotted on a line graph. The entire procedure was repeated for the 3, 5, 7, and 9 wt% of 0.125 g urea treated N-TiO_2 filled resin discs.

4.7. Investigating the effects of visible light on the colour of N-TiO_2 filled resin

Materials and equipment

- Dental curing light, CU 100A, TPC Advanced Technology, California, USA
- Desk lamp with a standard LED daylight light bulb, 6500K, 220-240V, Anglepoise laboratories, UK
- Shade guide, VITA classical A1-D4, VITA Zahnfabrik, Germany

Methods

In this section, visible light from an LED light source and a dental curing light were applied to the surface of the resin discs. This experiment was done on one unpolished sample 0.125 g urea treated N-TiO_2 filled resin at each wt% (Table 4). Each sample was placed on a flat surface and a desk lamp with a standard LED light source placed directly above at 2000 lux for 30 seconds. The samples were immediately compared with a shade guide under natural sunlight and any change in colour after light exposure was recorded with a digital camera.

The steps above were repeated with a dental curing light on a new set of samples. The dental curing light emits a different wavelength within the visible light region and is used clinically. Therefore, to investigate the effect of the colour change that could occur on exposure to the dental curing light, the blue light source was placed as close as possible to the surface of the resin sample, but without touching, for 30 s simulating the placement of the light clinically. Any change in colour was compared immediately after light exposure with a shade guide, under natural sunlight, by the same observer.

Experiment	Number of Samples					Readings per sample	Repeats
	Wt%	Surface Treatment					
		A	B	C	D		
4.5	1	2	2	2	2	-	-
	3	2	2	2	2	-	-
	5	2	2	2	2	-	-
	7	2	2	2	2	-	-
	9	2	2	2	2	-	-
4.6	1	1	1	1	1	3	2
	3	1	1	1	1	3	2
	5	1	1	1	1	3	2
	7	1	1	1	1	3	2
	9	1	1	1	1	3	2
4.7	1	1	-	-	-	-	2
	3	1	-	-	-	-	2
	5	1	-	-	-	-	2
	7	1	-	-	-	-	2
	9	1	-	-	-	-	2
4.8	0	9	9	9	9	3	2
	1	9	9	9	9	3	2
	3	9	9	9	9	3	2
	5	9	9	9	9	3	2
	7	9	9	9	9	3	2
	9	9	9	9	9	3	2

Table 4. The materials, number of samples at different wt%, surface treatments, spectrophotometer readings and repeats (light and dark) for experiments 4.5, 4.6, 4.7, and 4.8 (A-unpolished resin disc, B-Plasma treated resin disc, C-Polished only resin disc, and D-Polished and Plasma treated resin disc). In each case the N-TiO_2 filled resin disc was made using 0.125 g of urea.

4.8. Testing antibacterial properties

The reduction of Rhodamine B dye under visible light conditions showed that TiO_2 when calcined with urea at a high temperature can produce a powder with enhanced photocatalytic properties. However, what was still uncertain at this stage was whether or not the reactive oxygen species released were sufficient to have an effect on the growth of cariogenic oral bacteria, such as *S. mutans*. The potential antimicrobial properties of N-TiO_2 filled dental resins, at different wt% and surface treatments against *S. mutans* were tested as follows.

The antibacterial activity of the resin discs was assessed by quantifying the viability of the bacterial cells attached to the disc. Bacterial viability was quantified by a colorimetric method using tetrazolium salts (XTT reduction assay, (2,3-Bis-(2-Methoxy-4-Nitro-5-Sulfophenyl)-2*H*-Tetrazolium-5-Carboxanilide). The metabolically active cells cleave the salt to form formazan dye (orange in colour) and this dye can then be quantified directly using spectrophotometry. The change in the colour is considered proportional to the number of metabolically active cells (therefore, live cells).

The number of disc samples used, surface treatments, and repeats conducted in experiments 4.8.1, 4.8.2, and 4.8.4 are outlined in Table 4.

<u>Materials and equipment</u>

- *S. mutans* frozen stock UA159, University of Bristol, UK
- Frozen XTT stock (1 mg/mL), University of Bristol, UK
- Brain Heart Yeast broth (BHY)

- Sterilised deionised water
- Tweezer
- 24-well cell culture plate
- Phosphate buffer solution (PBS)
- 30ml Falcon tubes, Fisher Scientific UK Ltd, Loughborough, UK
- Acetone reagent, Sigma-Aldrich, Gillingham, Dorset, UK
- Menadione, Sigma-Aldrich, Gillingham, Dorset, UK
- Eppendorf tubes, Fisher Scientific UK Ltd, Loughborough, UK
- Research micropipette. Eppendorf UK Ltd, Stevenage, UK
- Lux light meter, DVM1300, Velleman, Gavere, Belgium
- Hotplate stirrer, Stuart US152, Bibby Scientific, Staffordshire, UK
- Autoclave steriliser, Omega Media, Prestige Medical Ltd, Blackburn, UK
- Centrifuge, Rotina 380r. Hettich lab technologies, Massachusetts, USA
- Desk lamp with a standard LED daylight light bulb, 6500K, 220-240V, Anglepoise laboratories, UK
- Cell density measurer, WPA Biowave, Biochrom, Cambridge, UK

4.8.1. Sterilising N-TiO_2 resin discs

Resin discs filled with 0,1,3,5,7, and 9 wt% of 0.125 g urea treated N-TiO_2 powder were prepared. These discs were subjected to the different surface treatments as described previously.

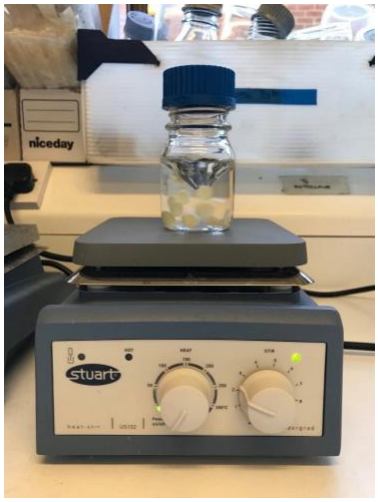

Figure 4. Sterilisation of resin discs.

Prior to antimicrobial testing, the discs were sterilised in a 200 ml glass bottle containing 150 ml of 70% ethanol solution under stirring conditions, set at mark 2, for 2 minutes. The discs were then washed by stirring them in sterilised distilled water for a further 2 minutes at the same speed. This washing process was repeated twice. Following this, the discs were then taken to the flow hood, which was initially sprayed with 70% ethanol and left to airdry for a few hours with the lid uncapped.

4.8.2. Antimicrobial testing of N-TiO_2 filled resin discs

S. mutans was taken from the freezer in the Oral Microbiology Department at Bristol Dental School and left to thaw at room temperature. Once completely thawed, 10 µl of the stock was dispensed into a 30 ml universal bottle containing 15 ml of BHY broth and incubated anaerobically for 18 hours at 37^{o}C for the bacteria to grow.

The following day, the inoculated broth was transferred into a 50 ml centrifuge tube and centrifuged for 5 minutes (20^{o}C, 5000 rpm). After 5 minutes, the supernatant was discarded and 5ml of PBS was added to the pellet and resuspended. This wash process was repeated twice. After the final wash, the bacterial pellet was resuspended in 5 ml of BHY. Once suspended, the solution was titrated into an orange capped Perspex tube containing BHY broth and the optical density of the suspension was adjusted for 0.8 at 600 nm. A higher cell count as depicted by optical density 0.8 was used to provide a maximum number of cells to be attached to the discs within 1.5 hours, allowing a measurable effect to be obtained via XTT reduction assay.

Two 24-well cell culture plates were prepared. One plate was to be exposed to visible light and the other kept in the dark. Nine unpolished samples (surface treatment A) of 0.125 g urea treated N-TiO_2 at 1 wt% resin discs were placed in the separate wells of each culture plate. A micropipette was used to transfer 500 µl of the *S. mutans* suspension to each well containing the resin samples. Both plates were incubated aerobically in the dark for 1.5 hours at 37^{o}C.

After the incubation, the supernatant was removed, and the discs were washed twice with 1 ml of PBS to remove any unattached cells. After the second wash, 500 µl of fresh BHY was added to each well to provide fresh nutrients for the attached bacterial cells. The first culture plate was incubated under visible light at 2000 lux at room temperature and pressure for 4 hours (Figure 5). The second plate was kept at room temperature and pressure under dark conditions for 4 hours by covering the plate with aluminium foil.

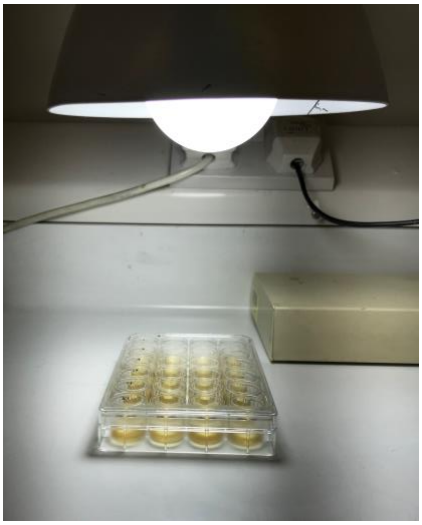

Figure 5. Exposure of resin samples +/- bacteria in BHY media to LED light for 4 hours at 2000 lux.

4.8.3. XTT dye solution preparation

While the well plates were left exposed to light and dark respectively for 4 hours, the XTT dye was prepared. Frozen XTT stock was thawed. Since XTT is sensitive to light, aluminium foil was used to cover the tube. Seven mg of menadione powder was dissolved in 1ml of acetone to produce 4000 µM of menadione solution. The tube was shaken by hand until the menadione was completely dissolved and diluted in sterile distilled water to produce a concentration of 40 µM. This final concentration of 40 µM menadione solution was used to prepare the dye. The final reaction solution of XTT was prepared by mixing 2 ml of XTT stock, 7.9 ml of PBS and 400 µl of freshly prepared 40 µM menadione solution.

4.8.4. Viability of *S. mutans* measurement by XTT assay

After 4 hours of exposure to visible light and dark respectively, each sample was carefully removed from the BHY medium with a pair of sterilised tweezers. Each disc was held on either side of the non-flat surfaces, and gently dipped into 1 ml of sterile PBS in a 24-well

plate. This process was done to remove any excess BHY on the disc without agitating the bacteria on the surface. Once the wash was done, the discs were then transferred into a clean 24-well plate. A micropipette was used to transfer 0.5 ml of the prepared XTT reaction solution to each well containing the disc bearing the grown bacterial cells and was left incubated aerobically at 37^{o}C for 1 hour in the dark. After 1 hour, 0.2 ml of all the solutions from each well were transferred onto a 96 flat-bottomed well plate and the absorbance was measured using a microplate reader (iMark Microplate Reader, Bio-Rad) at 490 nm wavelength.

This was repeated for the 0.125 g urea treated N-TiO_2 resin disc samples with surface treatments B, C, and D at 3,5,7, and 9 wt% as per methods outlined in section 4.8.2, 4.8.3, and 4.8.4.

5. RESULTS

5.1. Manufacture of N-TiO_2 powder

The manufacture of the N-TiO_2 powder via calcination of urea and TiO_2 at high temperature was carried out according to the protocol of Monteiro *et al.* (2015), starting with the manual grinding of the two powders together using just a pestle and mortar. However, even after 5 minutes the mixture produced was not thoroughly homogenous. Therefore, a Speedmixer containing zirconia balls was used for just 3 minutes at 2000 rpm in order to produce a more uniform mixture. Initially, the mixing time was set for 5 minutes, but this produced a powder that was dark yellow in colour. The most likely reason for this yellowing was the high mechanical energy generated when mixing for more than 4 minutes, initiating a reaction between the urea and TiO_2.

Following calcination, agglomeration of the resultant powder in the crucible meant further grinding was required to create a powder with sufficient surface area to enable it to display photocatalytic activity.

Figure 6 shows each of the N-TiO_2 powders produced following calcination. It can be seen that as the urea loading increased, so the powder became yellower and darker in colour when compared to the undoped TiO_2. Despite this change in colour, it was not considered to be sufficient to affect their potential use for aesthetic purposes. When exposed to ambient light, at room temperature and pressure, no subsequent change in colour was noted.

Figure 6. Examples of the N-TiO_2 powders produced following calcination. From left to right: undoped TiO_2, 0.125 g, 0.250 g, 0.375 g and 0.5 g urea treated TiO_2.

5.2. UV/Vis spectrometry of undoped TiO_2 and N-TiO_2 powders

A line graph plotted from the readings obtained from the UV/Vis spectrophotometer shows the reflectance of the undoped TiO_2 and the different N-TiO_2 powders at wavelengths between 200 and 500 nm (Figure 7).

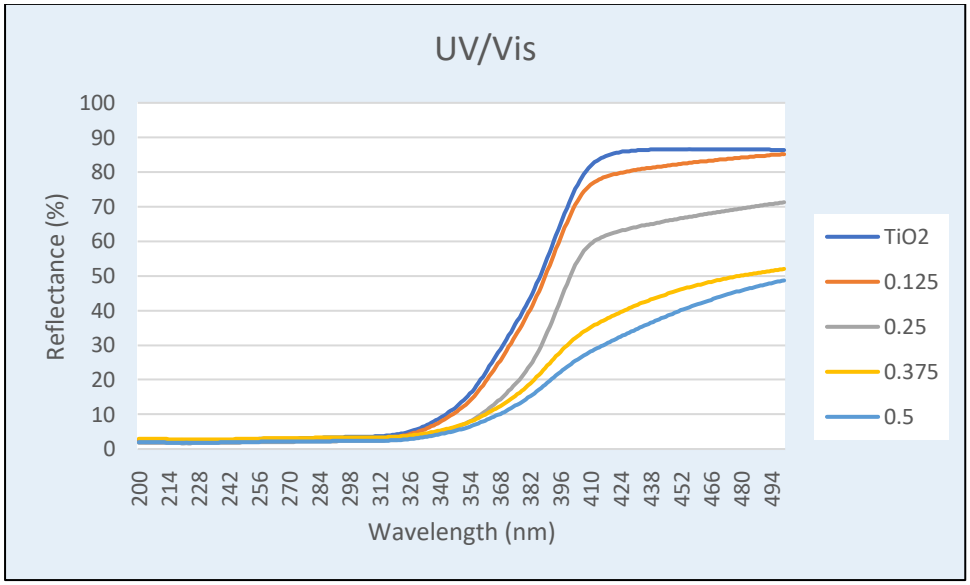

Figure 7. UV/Vis spectrometry readings for each of the undoped TiO_2 and N-TiO_2 powder with increasing urea loadings (0.125 to 0.5 g).

It can be seen that the overall trend was similar for all the samples. For the undoped TiO_2, the reflectance started with a baseline value of 2.69% at 200 nm. No change in reflectance was observed between 200 and 312 nm. A further increase in wavelength resulted in a sharp reflectance increase by 65.7%, reaching 86.5% at 417 nm. A plateau was observed as the wavelength continued to increase from 417 to 500 nm.

For the sample treated with 0.125 g urea, no change in reflectance was again observed between 200 and 312 nm wavelength. There was a sharp increase in reflectance between 312 and 417 nm before changing to a slow increase to reach a maximum value of 86.5% at 500 nm.

Similarly, for the samples at 0.25, 0.375 and 0.5 g urea loading, the reflectance remained fairly constant at 2.69% between 200 and 312 nm. The trend remained the same whereby a rapid increase in reflectance was observed until 417 nm, although by varying amounts depending on the nitrogen loading. This was followed by a slow increase until 500 nm was reached. From the graph, it was observed that the 0.25, 0.375, and 0.5 samples showed an increase in reflectance by 46, 49, and 68% respectively.

On increasing the nitrogen content, the reflectance spectrum was subjected to a red shift towards the visible light region. For example, at 30% reflectance, light of longer wavelengths was absorbed rather than reflected by the N-TiO_2 powders compared to the undoped TiO_2.

5.3. Calculation of band gap using Tauc plots

A Tauc plot is a method commonly used for the measurement of band gaps. The following mathematical expression suggested by Tauc (1968) was used:

$$(h\nu\alpha)^{1/n} = A(h\nu - Eg)$$

Where:

h: Planck's constant

v: Frequency of vibration

α: Absorption coefficient

Eg: Band gap

A: Proportional constant

The value of n denotes the nature of the sample transition. Since indirect allowed transition was used in this experiment, n=2 was used in the calculation.

The reflectance was analysed by converting the reflectance readings using the Kubelka-Munk function given as $F(R_\infty)$ (Tauc, 1968). This function is directly proportional to the absorption coefficient, α. α in the Tauc equation is substituted with $F(R_\infty)$, and therefore the equation becomes:

$$(h\nu\, F(R_\infty))^{1/2} = A(h\nu - Eg)$$

Based on this equation, line graphs of (hv $F(R_\infty)$)$^{1/2}$ against hv for the undoped TiO_2 and N-TiO_2 with different urea loadings were plotted. The unit for hv is electron volts (eV). The band gap was determined from each line graph as the point of intersection at the x-axis by a line of best fit plotted on the steepest gradient from the Tauc plot (Figure 8). The calculated band gaps are shown in Table 5.

Sample	**Band Gap (eV)**
TiO_2	3.22
0.125	3.11
0.25	2.99
0.375	2.97
0.5	2.92

Table 5. Band gap energy for the undoped TiO_2 and N-TiO_2 at different urea loadings (0.125 to 0.5 g).

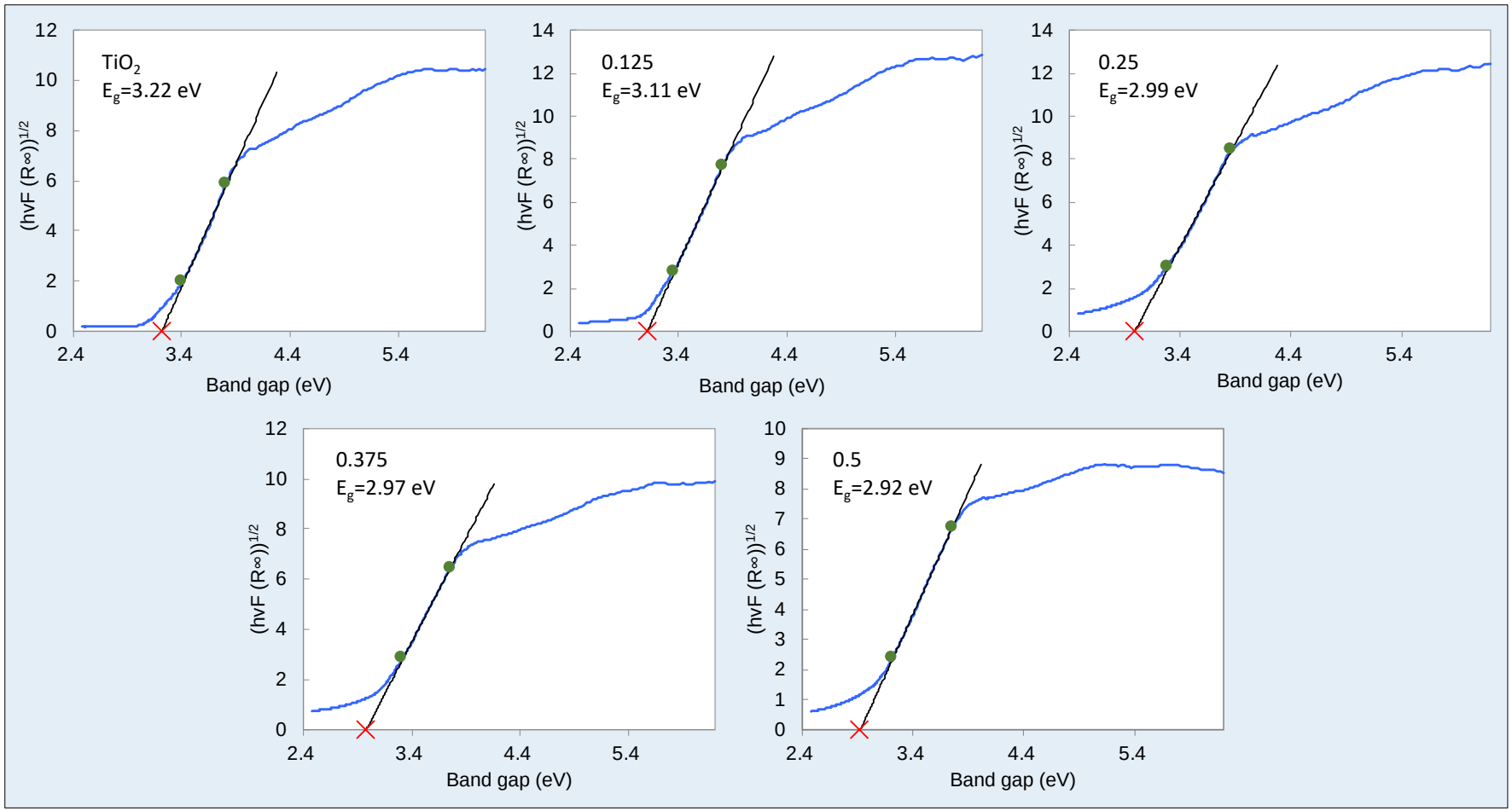

Figure 8. Tauc plots and band gap energy of undoped and N-TiO_2 powder at different urea loadings (0.125 to 0.5 g).

5.4. Investigation of the photocatalytic properties of TiO_2 and N-TiO_2 powder under light and dark conditions

In this experiment the photocatalytic properties of each of the different N-TiO_2 powders were investigated via their effect on Rhodamine B (Figure 9), along with the control undoped TiO_2 and also Rhodamine B with no powder added.

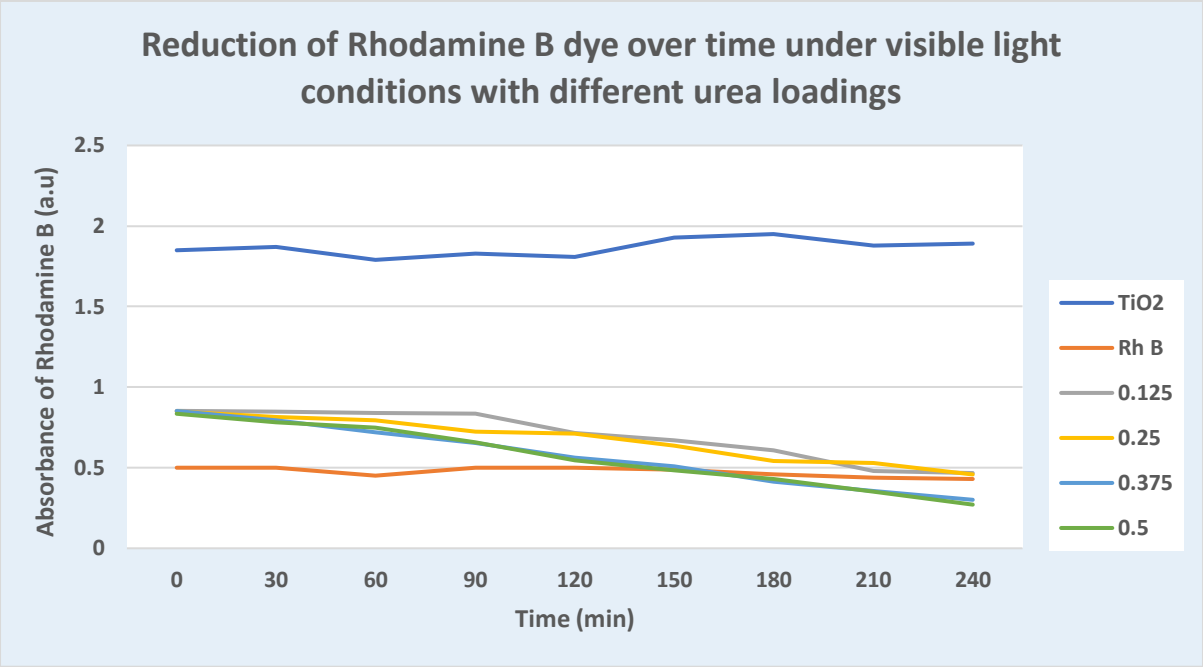

Figure 9. Absorbance (a.u.) over time under visible light conditions for N-TiO_2 with different urea loadings (0.125 to 0.5 g). Undoped TiO_2 and Rhodamine B (RhB) without the addition of a powder acting as the controls.

It can be seen that the Rhodamine B dye showed no reduction in absorbance over the 4-hour experimental period, with it remaining fairly constant at 0.45 a.u. Similarly, the undoped TiO_2 powder showed no obvious change, fluctuating slightly between 0.79 to 0.95 a.u. throughout the 4-hour period.

When looking next at the results for the four N-TiO_2 powders at 0 minutes, the absorbance was significantly lower at the start of the experiment than the undoped TiO_2 powder, and by 1.02 a.u.. Over the 4-hour experimental period this was then seen to reduce in each case, but by differing amounts. As the nitrogen doping of the powder increased (urea loading from 0.125g to 0.5g) the reduction in absorbance increased. After 4 hours of visible light exposure, samples with 0.125 and 0.25 g urea loadings reached absorbance values of 0.465 and 0.457 a.u. respectively, which were slightly above the Rhodamine B control at 0.432 a.u. By contrast, the samples with 0.375 and 0.5 urea loadings continued to drop lower than the absorbance of the Rhodamine B control to reach 0.302 and 0.271 a.u. respectively.

This experiment showed that TiO_2 powder when doped with nitrogen produced a compound that has photocatalytic properties under visible light conditions and that the sample with the highest urea loading of 0.5 g had the most effective reduction of Rhodamine B.

The same experiment was repeated under dark conditions to determine if the observed effects illustrated in Figure 9 were due to the photocatalytic activity of the N-TiO_2 powder. It can be seen in Figure 10, under dark conditions, there was no observed change in absorbance of the undoped TiO_2, N-TiO_2 or Rhodamine B dye only control. This was expected as TiO_2 in Rhodamine B dye only releases the reactive oxygen species under UV light conditions.

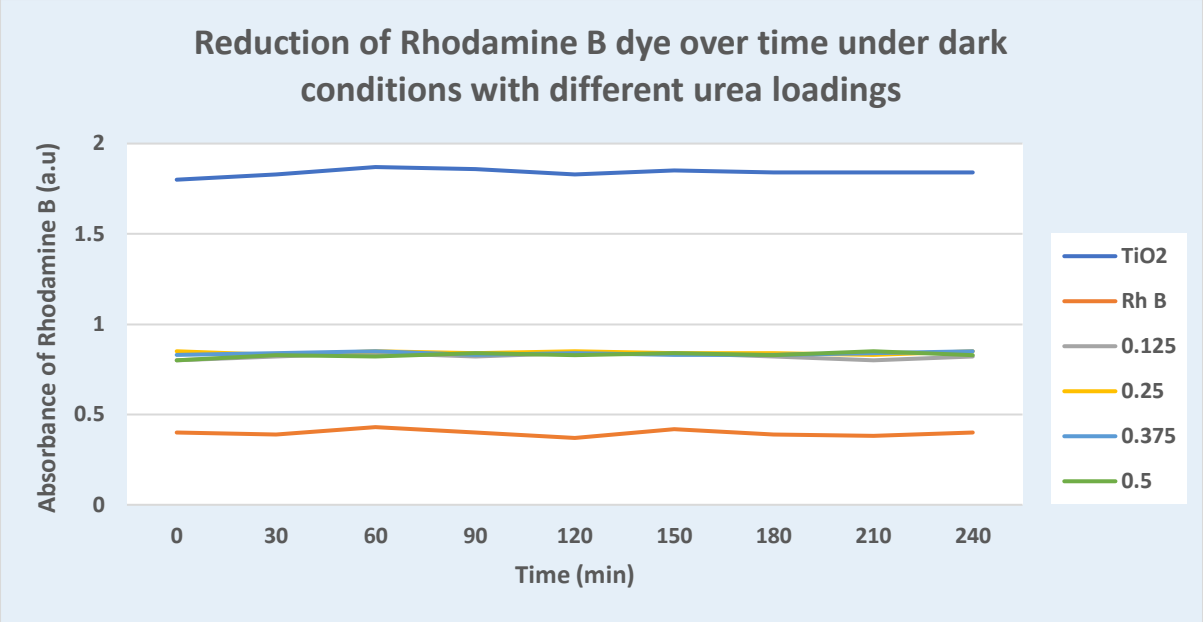

Figure 10. Absorbance (a.u.) over time under dark conditions for N-TiO_2 powder with different urea loadings (0.125 to 0.5 g). Undoped TiO_2 powder and Rhodamine B (RhB) without the addition of a powder acting as the controls.

5.5. Preparation of N-TiO_2 filled resin composite and colour assessment

In this experiment the effect of increasing the wt% of N-TiO_2 on the colour of TEGDMA/UDMA resins discs was investigated. Figure 11 shows the effect of increasing the wt% from 0 up to 9% N-TiO_2 powder created using 0.125 g urea loading.

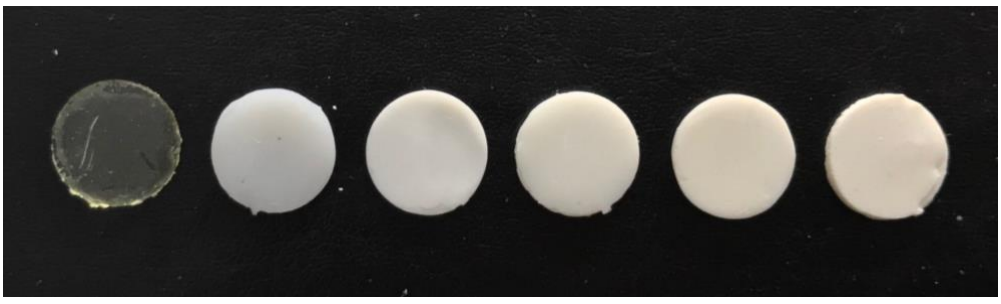

Figure 11. Unpolished TEGDMA/UDMA resin discs with increasing content of N-TiO_2 from left to right (0, 1, 3, 5, 7, 9 wt%). The initial urea loading was 0.125 g in each case.

It can be seen that increasing the content of powder from 0 to 9 wt% increased the yellowness and darkness of the set resin. During the fabrication of the resin discs the viscosity of the final mixed resin composite also appeared to increase with increasing powder content, although this was not formally tested. Sedimentation of the powder was also noted towards the base of the polyethylene jar and within approximately 10 seconds after mixing into the resin. Such settling of the powder at the base of the resin disc was considered a potential problem as it would affect the number of particles that would be exposed at the resin surface. To reduce this sedimentation effect, the silicone mould was immediately filled with the resin as soon as mixing was completed, and rapid setting was achieved by using a dental curing light.

Increasing the nitrogen content in the TiO_2 changed the colour of the resin from a pale yellow to a darker yellow with an underlying grey-ish hue. Even so, the aesthetic of the resin produced was comparable to the Vita Classic shade guide as seen in the picture below (Figure 12). The picture was taken immediately after the resin was cured. Each of the filled resin discs maintained the same shade even after 3 days post-curing.

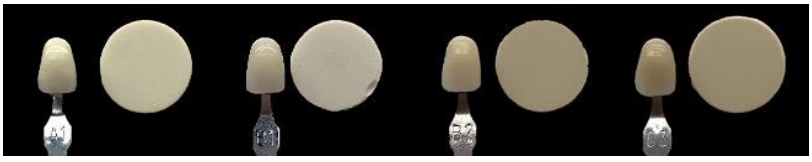

Figure 12. Colour comparison between Vita Classic shade guide and unpolished N-TiO_2 filled resin discs with increasing urea loading (0.125 to 0.5 g) at 9 wt%. From left to right; shade A1, 0.125 g urea treated N-TiO_2 disc, shade B1, 0.25 g urea treated N-TiO_2 disc, shade B2, 0.375 g urea treated N-TiO_2 disc, shade C3, 0.50 g urea treated N-TiO_2 disc.

5.6. Free radical release of N-TiO_2 filled resin at different nitrogen loadings with different surface treatments

To assess the effect of different concentrations and surface treatments on the photocatalytic activity of the nanofilled resin samples, the dental resin was incorporated with 1, 3, 5, 7, and 9 wt% of the 0.125 g urea treated N-TiO_2 powder and were subjected to surface treatments A unpolished, B unpolished but plasma treated, C polished, and D polished and plasma treated.

Figure 13 shows the reduction of Rhodamine B dye when 1 wt% of 0.125 g urea treated N-TiO_2 filled resin discs with four different surface treatments were exposed to visible light for 120 hours. Overall, there was a gradual decrease in absorbance over time for all surface treatments. After 120 hours, the unpolished sample (A) showed the least reduction, followed by unpolished plasma treatment (B), polished (C) and finally polished and plasma treated (D).

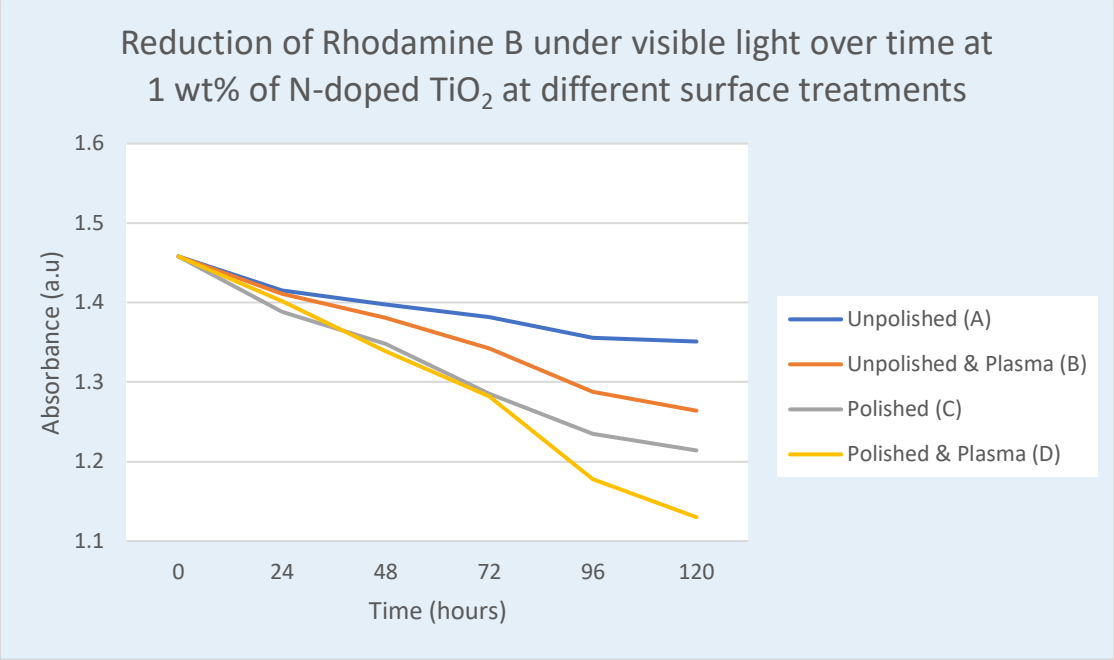

Figure 13. The effect of resin surface treatment on the reduction of Rhodamine B (RhB) dye under visible light over time at 1 wt% of 0.125 g urea treated N-TiO_2.

At 3 wt% of N-TiO_2 powder in resin the general trend of the graph showing reduction of Rhodamine B over time (Figure 14) similar to that seen with the 1 wt% specimens. Overall, there was a decrease in absorbance over time for all surface treatments. There was a steady drop in absorbance observed for surface treatments A, B, and D after 48 hours. By contrast, the absorbency started to decrease earlier, at 24 hours, for surface treatment C and was the lowest between 24 and 72 hours, before being overtaken by treatment D, as can be seen in the graph by the rapid drop in absorbance between 72 to 120 hours. After 120 hours, the reduction was greatest for treatment D, the polished and plasma treated sample, followed treatments C, B and A.

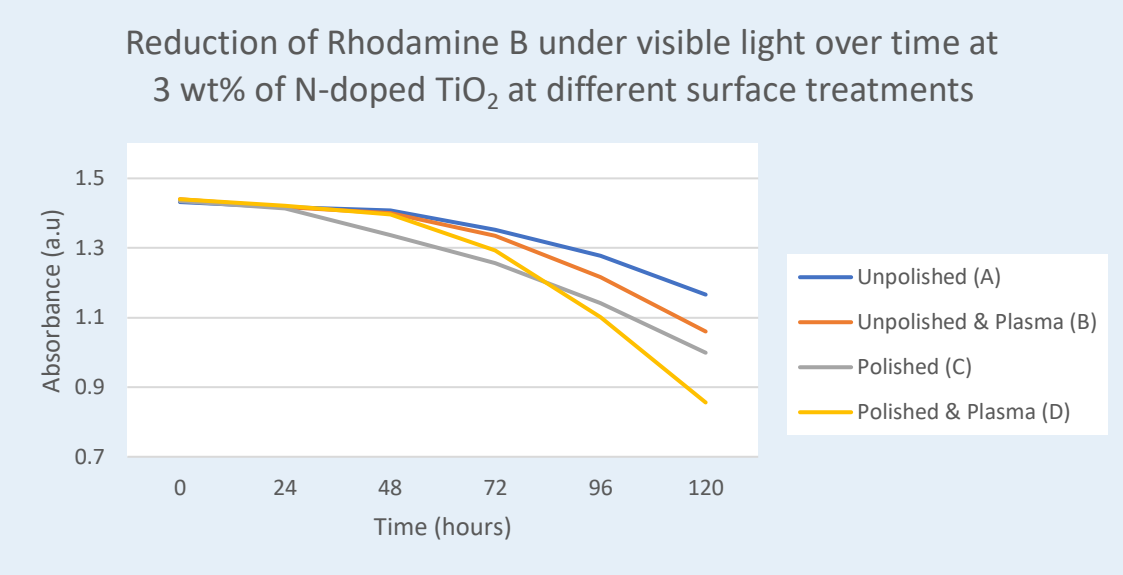

Figure 14. The effect of resin surface treatment on the reduction of Rhodamine B (RhB) dye under visible light over time at 3 wt% of 0.125 g urea treated N-TiO_2.

At 5 wt% of N-TiO_2 filled resin, the general trend showed there was a decrease in absorbance over time for all surface treatments (Figure 15). Between 0 to 24 hours, surface treatments C and D reduced the Rhodamine B dye at approximately the same rate. However, for treatment C between 24 to 48 hours, there was a rapid and unexpected increase in absorbency from 1.352 to 1.363 a.u before dropping sharply after 48 hours. Once again, after 120 hours of visible light exposure, surface treatment D showed the greatest reduction followed by C, B, and A.

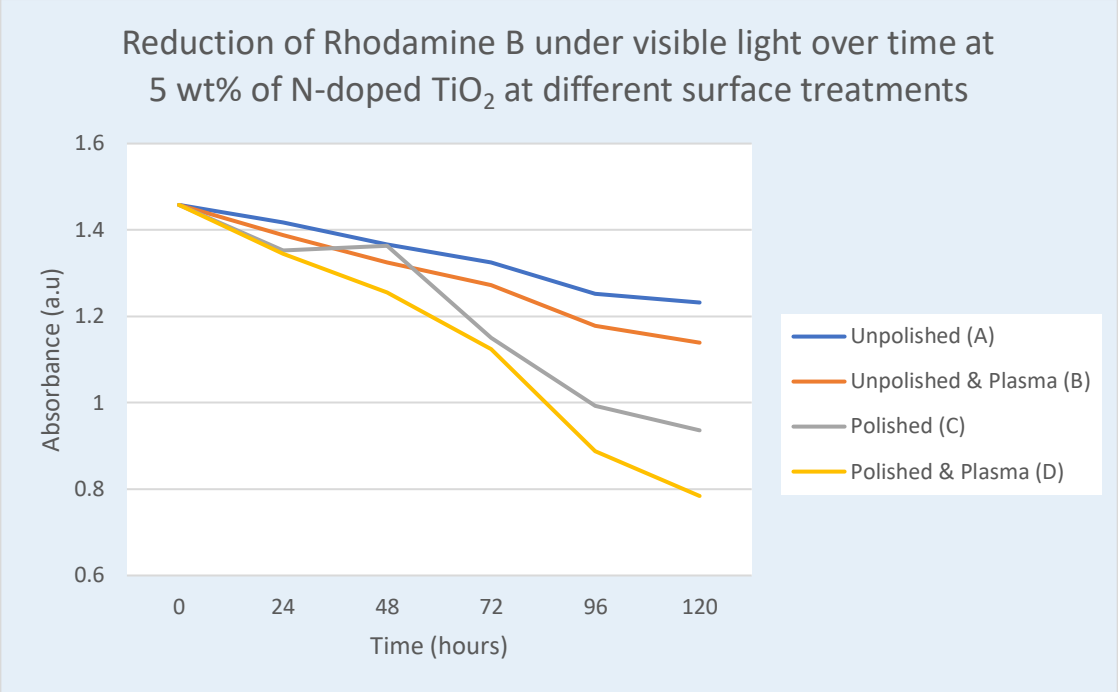

Figure 15. The effect of resin surface treatment on the reduction of Rhodamine B (RhB) dye under visible light over time at 5 wt% of 0.125 g urea treated N-TiO_2.

At 7 wt% of N-TiO_2 filled resin, the general trend showed there was a decrease in absorbency over time for all samples (Figure 16). Surface treatment A reduced more dye than B for the first 48 hours. However, the absorbance value for surface treatment B was lower than A between hours 48 to 120. Similar to the results obtained with the 1 wt%, 3 wt% and 5 wt% N-TiO_2 materials with the different surface treatments (Figures 13, 14 and 15), after 120 hours of visible light exposure, surface treatment D reduced the most dye followed by C, B, and A.

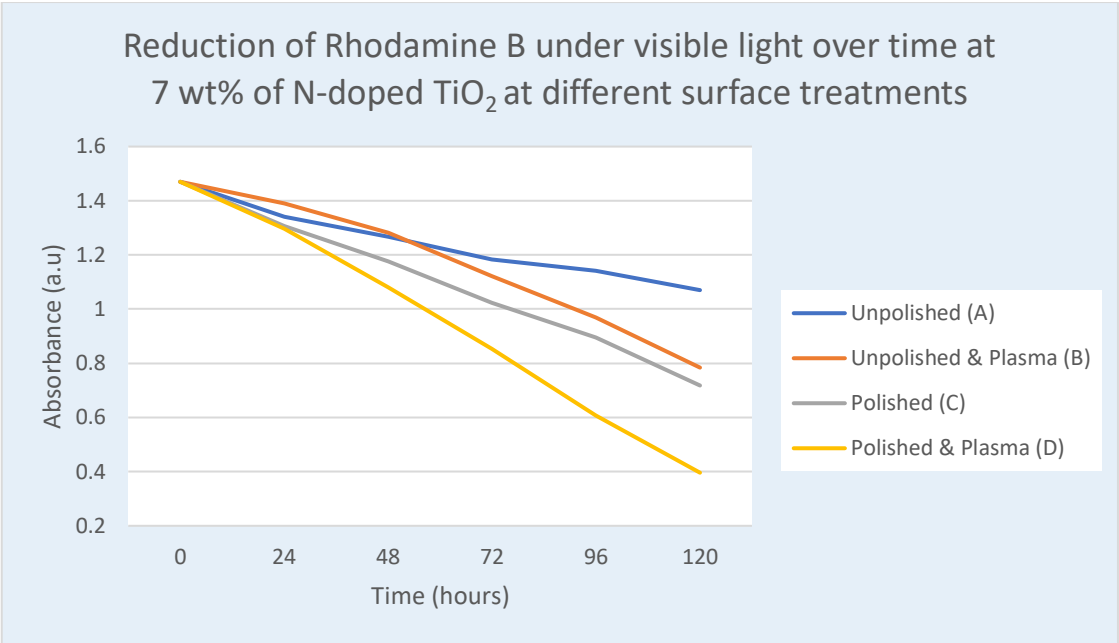

Figure 16. The effect of resin surface treatment on the reduction of Rhodamine B (RhB) dye under visible light over time at 7 wt% of 0.125 g urea treated N-TiO_2.

At 9 wt% of N-TiO_2 filled resin, there was a decrease in absorbance over time for all surface treatments (Figure 17). A rapid drop in absorbance can be observed for treatments A, B and C after 48 hours of visible light exposure, and even earlier at 24 hours for treatment D, polished and plasma treated. After 120 hours of visible light exposure, surface treatment D had the lowest absorbance value of 0.352 a.u. followed by C, B, and A with readings of 0.456, 0.656 and 0.789 a.u. respectively.

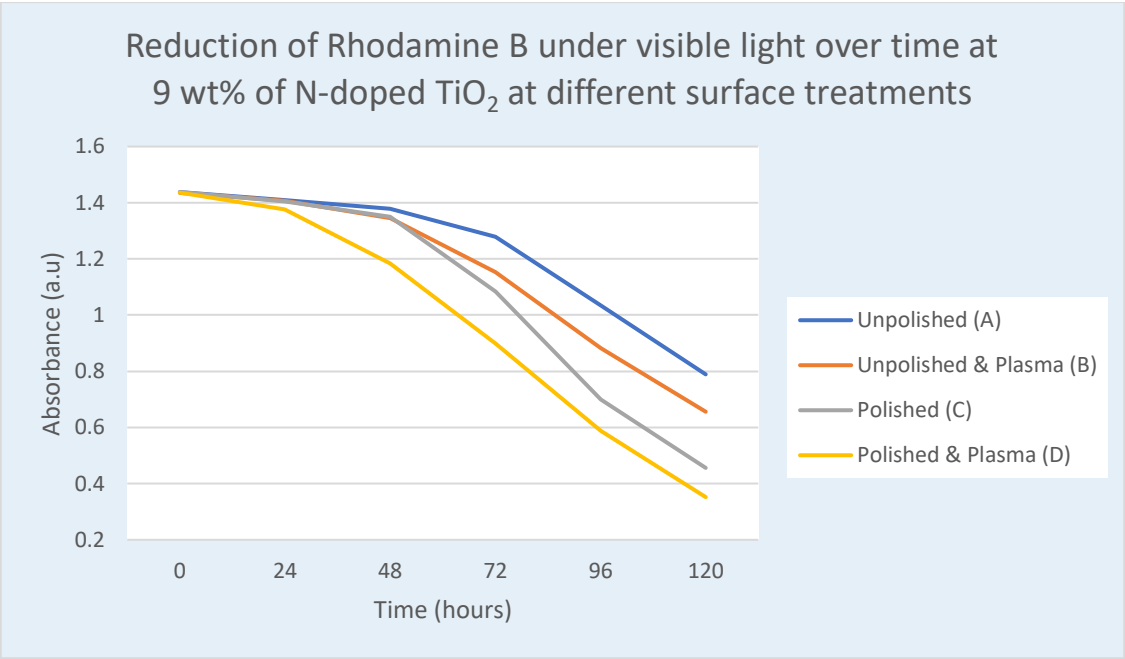

Figure 17. The effect of resin surface treatment on the reduction of Rhodamine B (RhB) dye under visible light over time at 9 wt% of 0.125 g urea treated N-TiO_2.

When the wt% of the 0.125 g urea treated N-TiO_2 is plotted against absorbance for each of the four surface treatments at 120 hours, as shown in Figure 18, it can be seen the reduction in absorbance increases with increasing wt%. This trend is seen with all four surface treatments but was greatest in the case of the polished plasma treated surface.

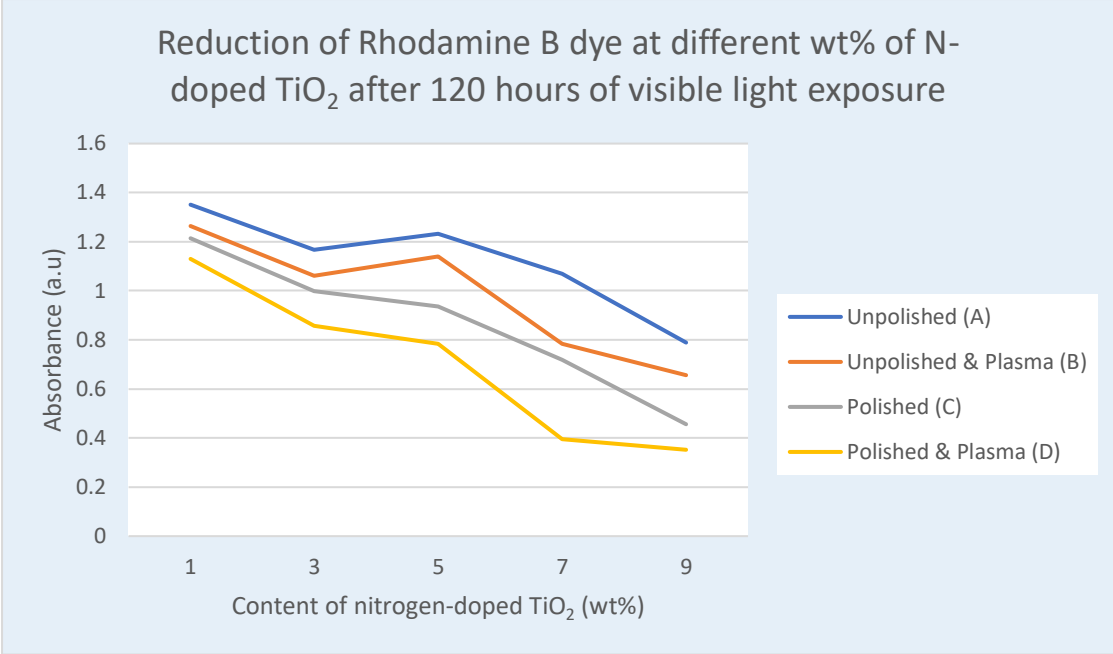

Figure 18. The effect of wt% on 0.125 g urea treated N-TiO_2 in the resin and surface treatment on the reduction of Rhodamine B (RhB) dye after 120 hours of visible light exposure.

5.7. Effects of visible light on N-TiO_2

One of the main concerns regarding the pilot experiment done by Chambers *et al.* (2014) was the colour change of the silver-doped TiO_2 filled resin discs from white to grey on exposure to visible light. This grey discolouration was considered to be an issue if this were to be used with aesthetic orthodontic brackets.

In the current study, following exposure to visible light for 30s at 2000 lux, no colour change was observed in any of the unpolished resin samples. By contrast, upon re-exposure to the blue light emitted by the dental curing light, a pale blue colour was observed on the surface of the exposed discs. This was of concern, as the discolouration could shine through if used with an aesthetic bracket. The intensity of the discolouration increased the higher the wt%

of the filler particles (Figure 19). Interestingly, the blue discolouration only lasted about 60 minutes for the resin containing 1 wt% filler before starting to gradually fade. A similar observation was found for the resin discs samples with filler particles at higher wt%, although it took longer for the discolouration to fade.

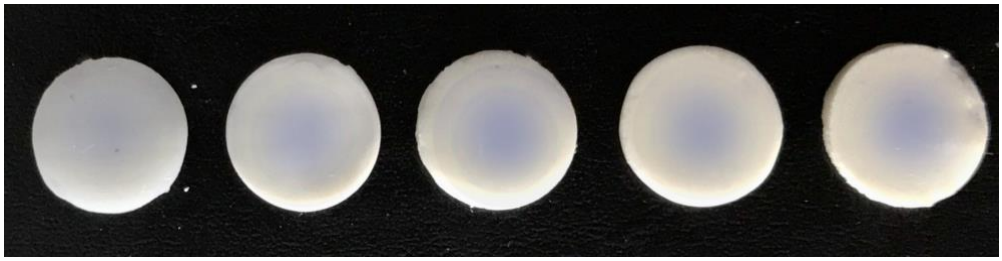

Figure 19. Discolouration on unpolished N-TiO_2 resin discs after 30 s exposure to a dental curing light. From left to right 1, 3, 5, 7, and 9 wt% 0.125 g urea treated N-TiO_2 filled resin discs.

5.8. Antibacterial properties of N-TiO_2 filled resin discs

The data on cell viability on contact with the resin surface was analysed using SPSS statistics package (IBM Corp, Armonk, USA) with a predetermined significance level of α=0.05. Summary statistics are presented as means, standard deviations, 95% confidence intervals of the mean, medians, maxima and minima (Table 6). The samples used were tested for normality using the Shapiro Wilks test and in most instances were found to be normally distributed. As a result, within each data set Student's *t*-test was used to compare the groups.

In the analysis of the dye using spectrophotometry the units are absorbance, which are directly proportional to the number of viable cells. Therefore, the lower the absorbance, the lower the number of viable cells on the surface of the resin.

Exposure	Content of N-TiO2 / wt%	Surface treatment	N	Mean	SD	Min	Max	95% CI		Shapiro Wilks (*P*>z)
Light	0	Unpol	9	0.071	0.003	0.068	0.074	0.069	0.073	0.040
Light	0	Plas	9	0.073	0.002	0.069	0.075	0.071	0.074	0.492
Light	0	Pol	9	0.072	0.001	0.071	0.073	0.072	0.073	0.055
Light	0	Pol & Plas	9	0.072	0.001	0.071	0.073	0.072	0.073	0.025
Light	1	Unpol	9	0.070	0.007	0.063	0.078	0.064	0.075	0.010
Light	1	Plas	9	0.068	0.006	0.061	0.075	0.063	0.073	0.015
Light	1	Pol	9	0.067	0.006	0.060	0.074	0.063	0.072	0.174
Light	1	Pol & Plas	9	0.066	0.005	0.060	0.073	0.063	0.070	0.391
Light	3	Unpol	9	0.067	0.003	0.063	0.071	0.064	0.069	0.136
Light	3	Plas	9	0.067	0.008	0.055	0.077	0.061	0.073	0.272
Light	3	Pol	9	0.057	0.004	0.051	0.061	0.054	0.060	0.024
Light	3	Pol & Plas	9	0.054	0.005	0.049	0.063	0.050	0.058	0.181
Light	5	Unpol	9	0.061	0.005	0.054	0.069	0.057	0.065	0.568
Light	5	Plas	9	0.060	0.004	0.054	0.065	0.057	0.064	0.089
Light	5	Pol	9	0.056	0.004	0.049	0.060	0.053	0.059	0.392
Light	5	Pol & Plas	9	0.048	0.006	0.040	0.058	0.043	0.053	0.414
Light	7	Unpol	9	0.059	0.005	0.053	0.067	0.055	0.063	0.456
Light	7	Plas	9	0.057	0.005	0.049	0.063	0.053	0.060	0.921
Light	7	Pol	9	0.052	0.004	0.046	0.057	0.049	0.055	0.448
Light	7	Pol & Plas	9	0.045	0.006	0.036	0.055	0.040	0.050	0.980
Light	9	Unpol	9	0.057	0.004	0.051	0.063	0.053	0.060	0.746
Light	9	Plas	9	0.055	0.005	0.048	0.062	0.051	0.059	0.433
Light	9	Pol	9	0.049	0.004	0.043	0.054	0.047	0.052	0.705
Light	9	Pol & Plas	9	0.042	0.005	0.035	0.048	0.038	0.046	0.154
Dark	0	Unpol	9	0.070	0.002	0.068	0.073	0.069	0.072	0.332
Dark	0	Plas	9	0.073	0.002	0.068	0.075	0.071	0.075	0.031
Dark	0	Pol	9	0.072	0.001	0.071	0.073	0.071	0.073	0.055
Dark	0	Pol & Plas	9	0.072	0.001	0.071	0.073	0.071	0.073	0.025
Dark	1	Unpol	9	0.068	0.002	0.066	0.071	0.067	0.070	0.255
Dark	1	Plas	9	0.071	0.004	0.067	0.079	0.068	0.074	0.072
Dark	1	Pol	9	0.069	0.002	0.066	0.071	0.067	0.070	0.011
Dark	1	Pol & Plas	9	0.067	0.003	0.065	0.072	0.065	0.069	0.064
Dark	3	Unpol	9	0.069	0.005	0.063	0.078	0.065	0.072	0.315
Dark	3	Plas	9	0.069	0.008	0.059	0.081	0.063	0.075	0.452
Dark	3	Pol	9	0.070	0.005	0.063	0.075	0.066	0.074	0.102
Dark	3	Pol & Plas	9	0.070	0.004	0.064	0.075	0.067	0.074	0.087
Dark	5	Unpol	9	0.068	0.005	0.058	0.074	0.065	0.072	0.233
Dark	5	Plas	9	0.070	0.004	0.063	0.075	0.066	0.073	0.427
Dark	5	Pol	9	0.065	0.003	0.060	0.069	0.063	0.067	0.735
Dark	5	Pol & Plas	9	0.061	0.003	0.056	0.065	0.059	0.063	0.767
Dark	7	Unpol	9	0.067	0.003	0.064	0.073	0.065	0.070	0.356
Dark	7	Plas	9	0.067	0.004	0.059	0.073	0.064	0.071	0.620
Dark	7	Pol	9	0.064	0.005	0.058	0.072	0.060	0.067	0.505

Dark	7	Pol & Plas	9	0.061	0.005	0.055	0.070	0.057	0.065	0.433
Dark	9	Unpol	9	0.065	0.003	0.061	0.070	0.063	0.068	0.333
Dark	9	Plas	9	0.065	0.004	0.059	0.070	0.061	0.068	0.374
Dark	9	Pol	9	0.062	0.003	0.059	0.067	0.060	0.065	0.159
Dark	9	Pol & Plas	9	0.061	0.003	0.058	0.065	0.059	0.063	0.382

Table 6. Summary data of the effect of light exposure, surface treatments (unpolished, polished, plasma treated, polished and plasma treatment), and different wt % (0-9 wt%) of 0.125 g urea treated N-TiO_2 powder on the absorbance presented as means, standard deviation, minima, maxima, standard error, 95% confidence intervals.

The bar charts (Figure 20) showed the effect of light exposure, surface treatments and N-TiO_2 at differing wt% content within the resin discs on the mean absorbance. On light exposure, as the powder concentration increased from 0 to 9 wt%, the absorbance fell by 8.4% for the unpolished samples followed by samples that were plasma treated, polished, and polished with plasma treatment with reductions of 24.7%, 31%, and 41.7% respectively. The results also showed that increasing the wt% of powder in the discs reduced the absorbance, with the lowest absorbance seen with the 9wt% of powder and the highest absorbance for the resin discs without any added powder for all surface treatments. There was a significant difference in absorbance between samples left in light and dark conditions for all surface treatments, but not for all wt%. Upon light exposure, the unpolished samples showed a significant reduction (p=0.05) in absorbance at 7 and 9 wt%, whereas the plasma treated samples showed a significant reduction at 5, 7, and 9 wt%. At 3, 5, 7, and 9wt%, light exposure had a significant effect on the absorbance for samples that were both polished and plasma treated. Overall, exposure to light and increasing the concentration of powder had the effect of reducing the absorbance for both untreated and treated surfaces.

The bar charts in Figure 21 show the absorbance observed for the resin disc samples exposed to different surface treatments at different wt% powder concentrations under light conditions. Overall, treating the surfaces of the resin discs had an effect in reducing the absorbance under light conditions, although by varying amounts.

At 0 wt% powder concentration, no obvious change in absorbance was observed between the different surface treatments. There was a reduction in absorbance for samples that were surface treated (plasma, polished, and polished with plasma treatment) at 1 wt%. However, this was not statistically significant (p=0.05) when compared with the untreated (unpolished) samples. As the powder concentration increased from 1 to 9 wt%, samples that had both surface treatments (polished and plasma) had the lowest absorbance value, whereas the untreated (unpolished) samples had the highest absorbance. The samples that were polished and that received both types of surface treatments (polished and plasma) had a significant absorbance reduction compared to the unpolished samples at 3, 5, 7, and 9 wt% powder concentration. Plasma treated samples also showed a reduction in absorbance at 1, 3, 5, 7, and 9 wt%. However, these reductions were not statistically significant.

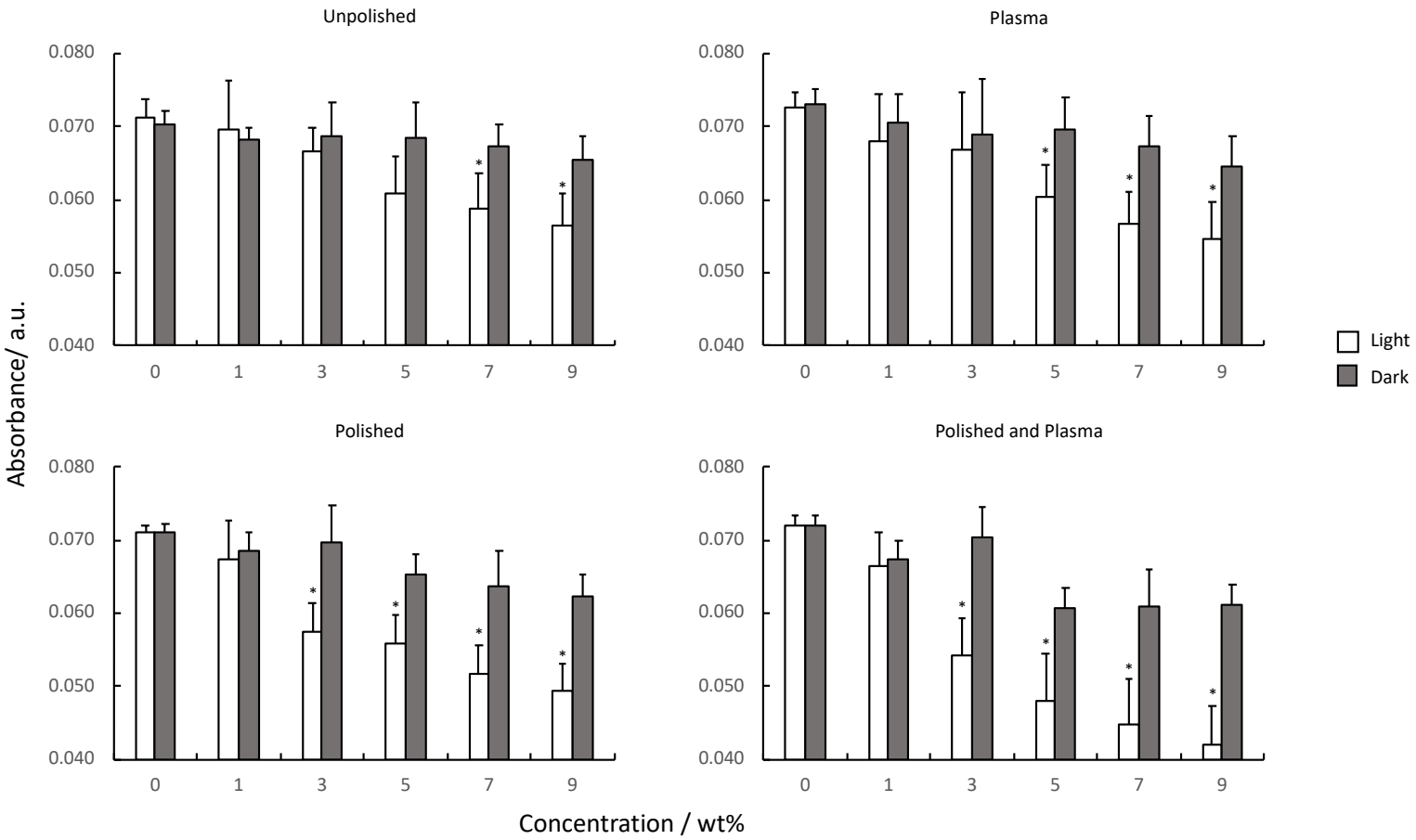

Figure 20. Bar charts of the absorbance observed for 0.125 g urea treated N-TiO_2 resin disc samples with different wt% powder concentrations (0-9 wt%), exposed to different surface treatments (unpolished, plasma treated, polished, and polished with plasma treatment) under light and dark conditions. The asterisks indicate statistically significant differences (p<0.05) between light and dark conditions of samples with the same wt% and surface treatment.

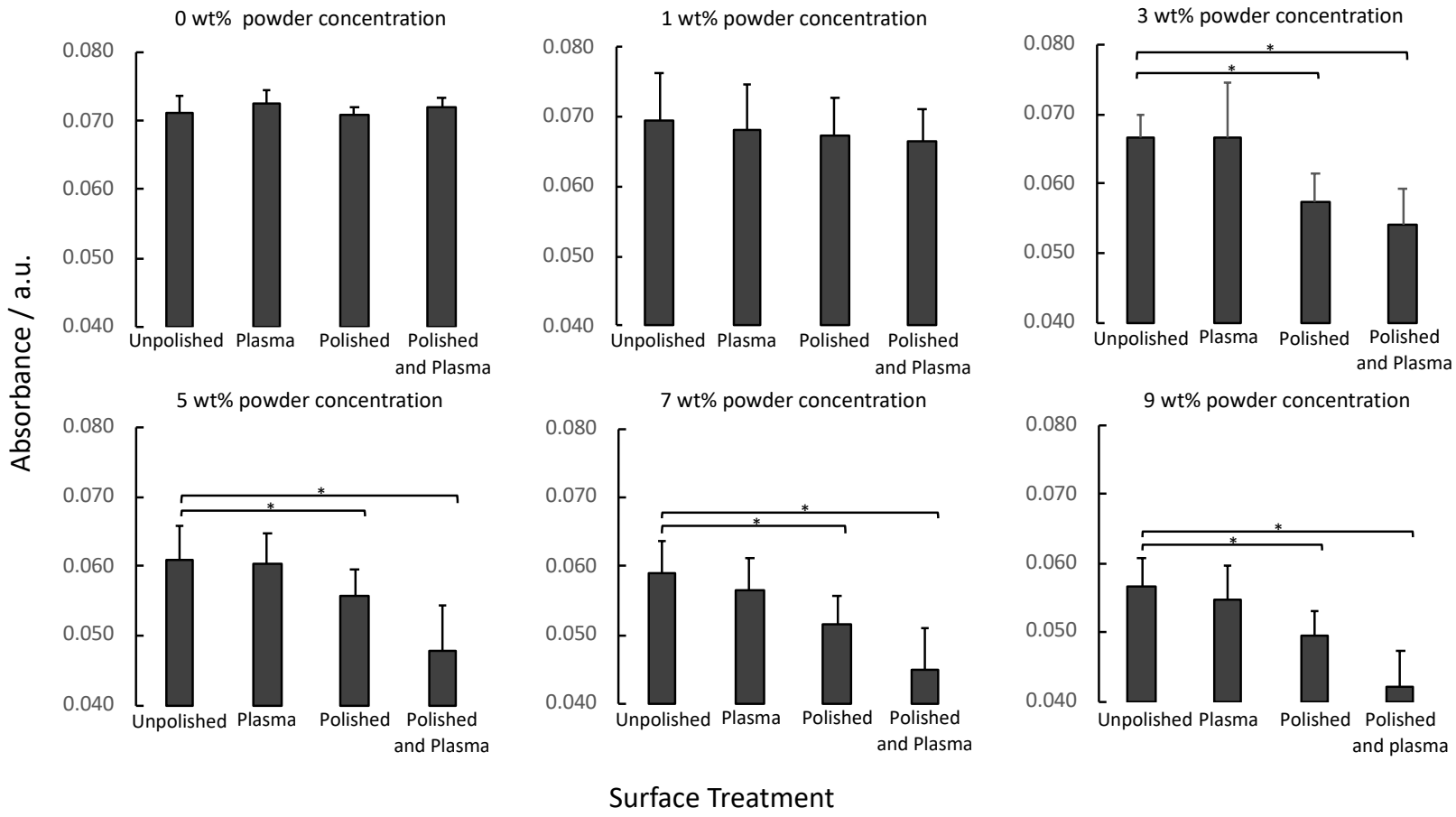

Figure 21. Bar charts of the absorbance observed for 0.125 g urea treated N-TiO_2 resin disc samples exposed to different surface treatments (unpolished, plasma treated, polished, and polished with plasma treatment) at different wt% powder concentrations (0-9 wt%) under light conditions. The asterisks indicate statistically significant differences (p<0.05).

6. DISCUSSION

Enamel decalcification and the methods used to reduce its incidence during orthodontic treatment has been the focus of considerable research in recent years (Ogaard *et al*., 2001; Brown *et al.,* 2011; Pithon *et al.,* 2015; Alabdullah *et al.,* 2017). Various non-compliance methods that have been developed to try to reduce the incidence of WSL amongst orthodontic patients, but with limited success. Limitations have included poor material aesthetics (Chambers *et al.,* 2014), lack of long term active agent release (Farret *et al.*, 2011), and minimal or no effect in reducing the incidence of WSLs (Doherty *et al.*, 2002).

A popular area in nanomaterials research is into the photocatalytic effects of TiO_2, particularly enhancing its properties within the visible light spectrum by doping with another element. With this in mind, the main purpose of the current study was to manufacture a resin bonding adhesive containing N-TiO_2 with antimicrobial properties that was also aesthetic and so could be used with aesthetic orthodontic brackets.

6.1. Manufacture of N-TiO_2 powder

The method of N-TiO_2 manufacture used in the present study was based on the protocol of Monteiro *et al.* (2015). Following mixing of the two powders, the urea was calcined with pure TiO_2 powder at a high temperature of 380°C. This temperature was sufficiently high to decompose the nitrogen precursor, such that the nitrogen could be incorporated in the structure of TiO_2 (Wu *et al.,* 2010). However, it was also sufficiently low to prevent a decrease in the visible light absorption properties of the final material due to the higher presence of anatase phase in the crystalline structure. The crystalline phases, anatase and

rutile, significantly affect the photoactivity of the TiO_2 with the rutile phase being less efficient in this respect than the anatase phase (Nasirian *et al.*, 2018).

At the very start of this research, the urea and TiO_2 powder were manually ground together using a pestle and mortar followed by the use of a Speedmixer to produce a homogenous mix. The presence of zirconia milling balls when using the Speedmixer prevented clumping of the TiO_2 particles. The process of grinding using a pestle and mortar followed by the Speedmixer is not only important to produce a homogenous mix, but also to promote the substitution of nitrogen at the oxygen lattice site within the TiO_2 structure (Devi *et al.,* 2012). At room temperature, free energy barriers that exist within the TiO_2 lattice prevent the nitriding reaction from taking place. However, by grinding the powders together, the free energy of the system is lowered as part of the mechanical energy of grinding was used to distort the lattice structure through the formation of oxygen defects. The oxygen defects increase the surface energy, which in turn decreases the activation energy sufficient for nitridation to occur. This diffusion of nitrogen generates the N-TiO_2. The resultant powder contains residual organic substances, which are then removed through combustion by calcining the powder at a high temperature.

6.2. Band gap shift of N-TiO_2 using UV/Vis spectrophotometry

Although the effect of nitrogen doping of TiO_2 nanoparticles on the photocatalytic activity of the TiO_2 is thought to be attributed to the modification of the morphology and lattice construction of TiO_2 nanoparticles (Asahi *et al.,* 2014), the precise process is not clearly understood. It is generally accepted that the mode of doping could be either substitutional, interstitial, or a combination of the two. Substitutional doping leads to surface modification

of the TiO_2 through the attachment of nitrogen by intermolecular forces and involves oxygen replacement. By comparison, interstitial doping is thought to affect the lattice structure of the TiO_2, as this requires the addition of the nitrogen into the TiO_2 lattice. The location of nitrogen within the TiO_2 structure is crucial to its role as a photocatalyst. Both substitutional and interstitial doping are thought to be essential in the reduction of the band gap of TiO_2 (Ansari *et al.,* 2016), and in moving it towards the visible spectrum of light.

The reduction in band gap levels decreases the photon energy required for electron transition (Asahi *et al.,* 2014). Therefore, the absorption spectrum shifts toward higher values (red shift) and the absorption peak intensities enter to the visible light spectrum. Trapped electrons rapidly react with their mobile counterparts. In this process, the activation energy will reduce and promote photocatalytic activity under visible light irradiation (Mrowetz *et al*., 2004). An enhanced photocatalytic capacity of TiO_2 in the visible light region is obtained as the recombination efficiency of the electron-hole pairs is suppressed due to the alteration of the lattice structure in the presence of nitrogen.

In the present study, the reflectance spectra of the N-TiO_2 and pure TiO_2 powders (Figure 7) were measured in the region of 200 to 500nm, which includes part of the visible spectrum (380-740 nm) (Starr, 2005). It can be seen that nitrogen doping of TiO_2 resulted in absorption reaching well into the visible wavelength spectrum. The degree of absorption was concentration dependent. Adding more nitrogen precursor resulted in increased visible light absorbance. Therefore, for these samples, the modification of TiO_2 with nitrogen resulted in a red shift of the absorbance region, which is consistent with the research published by both Livraghi *et al.* (2009) and Monteiro *et al.* (2015).

Diffuse reflectance UV/Vis was used to determine the absorbance of the solid powder as it cannot be measured directly. To calculate the band gap changes, the Kubelka-Munk function based on the work by Tauc (1968) was used to convert the readings to absorbance. Only then can the band gap values be calculated. As the nitrogen loading increased, the band gap values exhibited a tendency to red shift towards the lower wavelengths, which was in agreement with existing literature (Mekprasart *et al.* 2013).

6.3. Photocatalytic properties of TiO_2 and N-TiO_2 powders under light and dark conditions

In this study, the photodegradation of Rhodamine B dye by N-TiO_2 and undoped TiO_2 under visible light and dark conditions was investigated.

The Rhodamine B dye used in this experiment is a redox indicator and previous work has shown that N-TiO_2 can reduce Rhodamine B under visible light irradiation (Cong *et al.,* 2007; Asahi *et al.,* 2014; Ansari *et al.,* 2016). It is an organic, water-soluble dye that is used widely in biotechnology applications and usually comes in a powdered form. It is easily dissolved in water to produce a fluorescent pink solution. Upon exposure to a reducing agent, the pink dye will turn colourless. The photodegradation mechanism of Rhodamine B involves the removal of the ethyl groups and breakage of the double bonds in the benzene ring structure of the dye by the ROS produced by the N-TiO_2 particles. This leads to the degradation of the organic dye into smaller molecules to produce carbon dioxide and water (Yang and Yang, 2008).

At the beginning of the experiment, the N-TiO_2 powders in the Rhodamine B dye solution were left in the dark for 30 minutes to achieve an adsorption-desorption equilibrium. This is necessary in order to achieve saturation prior to investigating the potential photocatalytic activity of the N-TiO_2 (Pichat, 1986). If this is not done, then the decrease in concentration of the dye will be due to adsorption and photocatalytic degradation rather than due to photocatalysis alone, leading to inaccurate measurement of the photocatalytic effects of the material under test.

When looking at the results for the absorbance using the four different N-TiO_2 powders with differing initial urea loadings and therefore degrees of nitrogen doping (Figure 8), it is obvious that the starting absorbance for all N-TiO_2 samples were lower than the undoped TiO_2 powder. The lower initial absorbance values were due to the size of the powder particles. The undoped TiO_2 was finer than the N-doped powders (Rattanakam *et al.,* 2009), and therefore dissolved more readily in the dye solution. Nevertheless, this study not only demonstrated the photocatalytic activity of the N-TiO_2 powders, but also that it was more effective with increasing nitrogen loading. There was little difference in photocatalytic activity between the 0.375 g and 0.5 g urea treated powders. The control containing the undoped TiO_2 powder showed no obvious change in readings throughout the entire 4 hours under visible light exposure, as the photocatalytic oxidation process of TiO_2 is only activated by irradiation with UV light (Pawar *et al.*, 2018). The LED light source used in this study did not emit UV radiation sufficient to activate free radicals release. Similarly, no change in absorbance was noted for all the samples left in the dark, with the absorbance values remaining at about 0.85 a.u.. The dark conditions provided insufficient energy for the electrons to overcome the large band gap to produce any photocatalytic reaction. No light is

available to photogenerate the holes and electrons needed to degrade the Rhodamine B dye (Lee *et al.,* 2020). This result suggests that nitrogen doping of TiO_2 enhances the photocatalytic degradation of Rhodamine B under visible light conditions compared to undoped TiO_2, due to the reduced band gap energy.

Previous research, looking at the effect of nitrogen doping on photocatalytic activity towards diphenhydramine degradation, found that photocatalytic activity increases up to a certain concentration, before decreasing due to the incomplete decomposition of the large doping nitrogen precursor content in the TiO_2 matrix (Monteiro *et al.,* 2015). Although there was little difference in the photocatalytic activity of the 0.375 g and 0.5 g urea treated powders in the present study, the work of Monteiro *et al.* (2015) used concentrations up to 6 times higher than this when describing the same effect.

6.4. Manufacturing of N-TiO_2 filled resin composite

An issue from the study by Chambers *et al.* (2014), using silver doped TiO_2, was settling of the powder at the base of the resin discs. This was because chemically cured epoxy resin was used, which had to be left to cure overnight. In the current experiment it was therefore decided to use a light cured dental resin with two photoinitiators added, namely camphorquinone and 4-EDMAB. The disc samples were also smaller in this experiment, both in diameter and height, so that the bulk adhesive could be light cured rapidly throughout before any powder settling occurred.

The recipe of the resin that was used in this experiment was based on the work done by Karabela and Sideridou (2011), and consisted of the following:

- Diurethane dimethacrylate (UDMA)
- Triethylene glycol dimethacrylate (TEGDMA)
- Ethyl 4-(dimethylamino) benzoate (4-EDMAB)
- Camphorquinone (CQ)

TEGDMA has a watery consistency compared to the thick and viscous UDMA. Therefore, to ensure the photoinitiators were well incorporated and dispersed in the bulk resin, they were firstly mixed with TEGDMA. Once fully combined, UDMA and finally the N-TiO_2 powder were added to the mix and fully incorporated. It was decided that 3 minutes of mixing using the Speedmixer was enough to produce a well dispersed resin and powder mix. Initially, the mixture was spun for 5 minutes, but this generated a lot of heat that resulted in the colour of the N-TiO_2 powder in the resin turning an even darker shade of yellow. This was due to the high mechanical energy generated during mixing, which accelerated further the nitridation of the TiO_2, resulting in the change in colour (Yin *et al.,* 2003).

Once the N-TiO_2 filled resin discs had set, the aesthetics were observed immediately after and again 3 days later, but no further colour changes were noted. Increasing the wt% of powder in the resin from 0 to 9 wt% did not alter the colour of the resin discs but did alter the degree of opacity. Resin discs with a lower powder content, e.g. 1 and 3 wt% were more translucent, which was perhaps to be expected.

6.5. Photocatalytic properties of N-TiO_2 filled resin discs

One of the main objectives of this research was to produce an aesthetic N-TiO_2 filled resin composite capable of photocatalysis under visible light. From the Rhodamine B dye

reduction experiment, the powder appeared to become darker with increased nitrogen loading. In the case of the sample with 0.125 g urea treated N-TiO_2, it was chosen to be incorporated in the dental resin as it was the most aesthetic and produced the lightest pale-yellow colour out of all the other samples. In addition, the reduction of Rhodamine B dye by this sample may just be enough to produce a visible and effective photocatalytic effect when combined with an unfilled dental resin. As such, the 0.125 g was used throughout the rest of this study.

A concern during the investigation was whether sufficient free radicals would be released from the N-TiO_2 powder once incorporated into the dental resin discs. Theoretically, it might be expected that the photocatalytic efficiency would be reduced, as most of the N-TiO_2 powder would be encased within the bulk of the solid resin block rather than at the resin surface. Increasing the concentration of N-TiO_2 powder would therefore likely increase the number of particles per unit surface area exposed to the environment and thereby enhance the photocatalytic effect on the Rhodamine B dye. To test this, the concentration of N-TiO_2 powder in the discs was increased (1, 3, 5, 7, and 9 wt%). In addition, the effect of treating the resin surface was also investigated using four different surface treatments (unpolished, polished, plasma treatment, combined polishing and plasma treatment) to see if this would also affect the number of particles exposed and therefore the photocatalytic activity.

Clinically, the unpolished resin represents the light cured resin composite during bonding of orthodontic brackets. Surface treatment by mechanical polishing can be done clinically by running a bur around the orthodontic bracket margins where the bonding resin is exposed to the oral environment. Alternatively, it may happen as a result of toothbrushing, although

this would rely on patient compliance. Unlike mechanical surface polishing, plasma treatment provides an alternative method of surface modification that is less abrasive and target specific. Bombardment of the surface of a polymeric resin with ionised oxygen molecules under low pressure preferentially removes the organic resin components of any composite, while leaving the filler particles *in-situ* (Mueller *et al.,* 1993). In the current experiment, this would mean more N-TiO_2 particles were likely to be exposed following plasma treatment and would explain the greater reactivity of the plasma treated surfaces compared to the untreated surfaces. The idea of plasma application is not new. Plasma treatment has shown promise in other dental applications including implant surface modification, root canal disinfection, and tooth bleaching to name a few. However, to date no such treatments are currently available to be used clinically (Cha and Park, 2014; Ranjan *et al.*, 2017; Kim *et al.,* 2018) as research has only been done *in-vitro* and in the early stages of investigations.

Even though polishing and plasma treatment were found to be effective in enhancing photocatalytic in the current laboratory experiment, the practicality of polishing or plasma treating the thin composite layer underneath orthodontic brackets in the orthodontic clinic is questionable. Additional steps during bonding and later adjustment appointments would undoubtedly increase the overall time required and might not be readily accepted by the clinicians. However, the results of the present study were promising in that even at the lowest wt% of N-TiO_2 of filler in unpolished resin discs, sufficient free radical release was taking place to photodegrade the Rhodamine B dye, which is promising.

6.6. Effects of visible light on N-TiO_2 filled resin

In this experiment, a temporary colour change of the filled resin discs occurred when they were re-exposed to the blue light emitted by the dental curing light. In contrast, no colour change was observed on exposure to the visible light from a LED desk lamp. This is most likely due to the different intensity of the lights. The intensity of the light emitted by the dental curing light was greater than the LED desk lamp. Fortunately, the pale blue colour observed was only temporary and might even be seen as an advantage when applied clinically, as it would potentially allow any resin flash to be identified and removed easily during orthodontic bonding or debonding. The colour change can be explained by the photoreduction of Ti^{4+} in the N-TiO_2 structure to Ti^{3+} which gives the resin a blue discolouration (Xiong *et al.,* 2012). After the discontinuation of the blue light exposure oxidation of Ti^{3+} will occur and over time the blue colour disappears.

The idea of colour changing bonding agents is not new and current commercially available products include Blugloo composite by Ormco and Transbond Plus composite resin by 3M, Unitek. Prior to curing these adhesives are blue and pink respectively, but when a curing light is applied, they set and become a yellow white colour similar to many other dental composites. However, in the case of Bluegloo, if at the time of debond, following bracket removal, a curing light is again shone on the debonded tooth surface, any remnants of Bluegloo will turn blue once more, making their identification and subsequent removal easy. In the current experiment interestingly the colour change from pale yellow to blue was not observed during the initial setting of the unset resin composite with the dental curing light. It was only after the resin was set that the change in colour was noticed following re-exposure to the blue light.

6.7. Antibacterial testing of N-TiO_2 filled resin discs

The photocatalytic effects of TiO_2 on viable bacterial cells have been successfully evaluated using metabolic assay previously, and so the same approach was adapted for use in this study (Daula *et al.,* 2013; Gyorgyey *et al.,* 2016; Baby *et al.,* 2017; and Fatani *et al.,* 2017). This assay technique is based on a reduction of pale-yellow tetrazolium salt to a bright orange formazan dye by metabolically active cells. The cells produce mitochondrial dehydrogenase within their mitochondria, and it is this enzyme that facilitates the conversion of the tetrazolium to formazan. The intensity of the bright orange formazan is directly proportional to the number of viable cells on the surface of the resin and is quantified using a scanning multi-well spectrophotometer.

In this study, the growth inhibition of *S. mutans* by N-TiO_2 was calculated on the basis of the absorbance of the dye. The findings showed that as the wt% of the N-TiO_2 filled resin discs increased, reduction in cell viability was observed under visible light conditions for all surface treatments. These findings are consistent with the results obtained from the reduction of the Rhodamine B dye described in section 5.6, which showed that the photocatalytic properties of N-TiO_2 were not inhibited even after being enclosed in the resin matrix. A possible reason for this could be due to the resin block not being a fully enclosed system, whereby the presence of porosities within the resin matrix could potentially expose the nanoparticles to the environment (Balthazard *et al.,* 2014). Following attachment of bacterial cells on the resin surface, reactive oxygen species produced in response to light exposure will have reacted directly with the cell membranes of the bacteria, promoting lipid peroxidation and DNA damage (Cai *et al*., 2013). This in turn will affect membrane permeability leading to cell death. Cell death reduces the production of mitochondrial

dehydrogenase, which decreases the conversion of the tetrazolium salt to formazan, giving rise to a lower absorbance reading.

Under the dark conditions of this experiment, the absorbance was higher for the samples left in the dark for all wt % of N-TiO_2 filled resin and surfaces. This suggests that more viable *S. mutans* were attached to the surface of the discs when left in the dark.

As expected, surface treatment by polishing and plasma irradiation of the resin surfaces increased the amount of photocatalyst exposed at the surface of the discs, thus affecting the viability of cells that were in contact with the discs. The degree of reduction was greater for the discs that were mechanically polished rather than just plasma treated, suggesting that polishing the discs had a greater effect in enhancing the photocatalytic activity of the filled resin discs when compared to plasma.

The current study investigated and developed an aesthetic antimicrobial free radical releasing resin-based composite, which displayed properties that may eventually be useful in orthodontics, particularly with aesthetic orthodontic brackets as light is able to pass through them directly to the antimicrobial adhesive. Indeed, such materials might also be useful in other areas of dentistry, *e.g*. in the provision of anterior composite resin restorations and in the manufacturing of polymeric orthodontic brackets. This photoinduced release of reactive oxygen species could be activated not only by natural daylight, at the front of the mouth, but could also be activated by the dentist or orthodontist at routine visits using just a dental curing light. The release of reactive oxygen species would have antibacterial effects on the cariogenic bacteria around the bracket periphery and may

reduce the prevalence of WSLs. However, this would not be a substitute for maintaining a good standard of oral hygiene, as the presence of a dense layer of plaque layer over the composite may itself reduce light penetration and therefore activation of free radical release by the composite. At completion of fixed appliance orthodontic treatment, the ability of the dental curing light to turn the N-TiO_2 composite blue would be an added benefit aiding residual bonding composite removal.

7. CONCLUSIONS

The conclusions that can be drawn from this study are:

- Nitrogen doping of TiO_2 produced a compound with a reduced band gap that exhibited photocatalytic properties under visible light conditions.
- Increasing the nitrogen loading enhanced the photocatalytic activity of N-TiO_2.
- N-TiO_2 powder is pale yellow in colour, which when incorporated in resin produces an aesthetic adhesive composite material comparable to current commercially available dental composites.
- The photocatalytic properties of N-TiO_2 were still observed even after incorporation into dental resin.
- Mechanical polishing and plasma irradiation enhanced the photocatalytic properties of the N-TiO_2 filled resin discs.
- N-TiO_2 filled resin discs exhibited an antimicrobial effect when in contact with *S. mutans* under visible light exposure.

8. FURTHER WORK

Further work might include investigating:

- The effect of the N-TiO_2 particles, in particular different filler loading on the physical properties of the adhesive resin, including compressive and tensile strength.
- The minimum N-TiO_2 filler loading required to produce sufficient photocatalytic activity to maintain the antibacterial properties, without compromising the physical properties of the adhesive.
- This study was only limited to testing the antimicrobial effect on *S. mutans.* Therefore, it might be useful as a future study to look at the effects on other species of cariogenic bacteria, possibly also the inhibitory effect of N-TiO_2 on cariogenic biofilm formation as well as the behavior of N-TiO_2 filled resin on an orthodontic bracket in a simulated oral environment and or real-world representation.

9. REFERENCES

ABOU NEEL, E. A., BOZEC, L., PEREZ, R. A., KIM, H. W. & KNOWLES, J. C. 2015. Nanotechnology in dentistry: prevention, diagnosis, and therapy. *Int J Nanomedicine,* 10, 6371-94.

ABU-BAKR, N., HAN, L., OKAMOTO, A. & IWAKU, M. 2000. Changes in the mechanical properties and surface texture of compomer immersed in various media. *J Prosthet Dent,* 84, 444-52.

AHN, S. J., LEE, S. J., LIM, B. S. & NAHM, D. S. 2007. Quantitative determination of adhesion patterns of cariogenic streptococci to various orthodontic brackets. *Am J Orthod Dentofacial Orthop,* 132, 815-21.

AHN, S. J., LEE, S. J., KOOK, J. K. & LIM, B. S. 2009. Experimental antimicrobial orthodontic adhesives using nanofillers and silver nanoparticles. *Dent Mater,* 25, 206-13.

ALABDULLAH, M. M., NABAWIA, A., AJAJ, M. A. & SALTAJI, H. 2017. Effect of fluoride-releasing resin composite in white spot lesions prevention: a single-centre, split-mouth, randomized controlled trial. *Eur J Orthod,* 39, 6, 634-40.

AL-MUNAJED, M. K., GORDON, P. H. & MCCABE, J. F. 2000. The use of a cyanoacrylate adhesive for bonding orthodontic brackets: an ex-vivo study. *J Orthod,* 27, 255-60.

ANHOURY, P., NATHANSON, D., HUGHES, C. V., SOCRANSKY, S., FERES, M. & CHOU, L. L. 2002. Microbial profile on metallic and ceramic bracket materials. *Angle Orthod,* 72, 338-43.

ANSARI, S. A., KHAN, M., ANSARI, M. O. & CHO, M. H. 2016. Nitrogen-doped titanium dioxide (N-doped TiO_2) for visible light photocatalysis. *New J Chem*, 40, 3000-09.

ASAHI, R., MORIKAWA, T., IRIE, H. & OHWAKI, T. 2014. Nitrogen-doped titanium dioxide as visible-light-sensitive photocatalyst: designs, developments, and prospects. *Chem Rev,* 114, 9824-52.

ASMUSSEN, E. 1985. Clinical relevance of physical, chemical, and bonding properties of composite resins. *Oper Dent,* 10, 61-73.

BABY, R. D., SUBRAMANIAM, S., ARUMUGAM, I. & PADMANABHAN, S. 2017. Assessment of antibacterial and cytotoxic effects of orthodontic stainless steel brackets coated with different phases of titanium oxide: An in-vitro study. *Am J Orthod Dentofacial Orthop,* 151, 4,678-684.

BACSA, R. R. & KIWI, J. 1998. Effect of rutile phase on the photocatalytic properties of nanocrystalline titania during the degradation of p-coumaric acid. *Applied Catalysis B: Environmental,* 16, 19-29.

BALENSEIFEN, J. W. & MADONIA, J. V. 1970. Study of dental plaque in orthodontic patients. *J Dent Res,* 49, 320-4.

BALTHAZARD, R., JAGER, S., DAHOUN, A., GERDOLLE, D., ENGELS-DEUTSCH, M. & MORTIER, E. 2014. High-resolution tomography study of the porosity of three restorative resin composites. *Clin Oral Invest,* 18, 6, 1613-18.

BANERJEE, A., WATSON, T., KIDD, E. & PICKARD, H. M. 2003. Restorative materials and their relationship to tooth structure. *Pickard's Manual of Operative Dentistry.* 9th Ed. London: Oxford University Press, 87-100.

BAYAT, J. T., HUGGARE, J., MOHLIN, B. & AKRAMI, N. 2017. Determinants of orthodontic treatment need and demand: a cross-sectional path model study. *Eur J Orthod,* 39, 85-91.

BENSON, P. E., PARKIN, N., DYER, F., MILLETT, D. T., FURNESS, S. & GERMAIN, P. 2013. Fluorides for the prevention of early tooth decay (demineralised white lesions) during fixed brace treatment. *Cochrane Database Syst Rev*, CD003809.

BENSON, P. E., SHAH, A. A., MILLETT, D. T., DYER, F., PARKIN, N. & VINE, R. S. 2005. Fluorides, orthodontics and demineralization: a systematic review. *J Orthod,* 32, 102-14.

BHARDWAJ, A., MISURIYA, A., MAROLI, S., MANJULA, S. & SINGH, A. K. 2014. Nanotechnology in dentistry: Present and future. *J Int Oral Health,* 6, 121-6.

BISHARA, S. E. & FEHR, D. E. 1997. Ceramic brackets: something old, something new, a review. *Semin Orthod,* 3, 178-88.

BISHARA, S. E., FONESCA, J., FEHR, D. & BOYER, D. 1994. Debonding forces applied to ceramic brackets simulating clinical conditions. *Angle Orthod,* 64, 277–82.

BORZABADI-FARAHANI, A., BORZABADI, E. & LYNCH, E. 2014. Nanoparticles in orthodontics, a review of antimicrobial and anti-caries applications. *Acta Odontol Scand,* 72, 413-7.

BRADWAY, S. D., BERGEY, E. J., JONES, P. C. & LEVINE, M. J. 1989. Oral mucosal pellicle. Adsorption and transpeptidation of salivary components to buccal epithelial cells. *Biochem J,* 261, 887-96.

BRAGA, R. R. 2019. Calcium phosphate as ion-releasing fillers in restorative resin -based materials. *Dent Materials,* 35, 3-14.

BROWN, M. L., DAVIS, H., TUFEKCI, E., CROWE, J. J., COVELL, D. A. & MITCHELL, J. C. 2011. Ion release from a novel orthodontic resin bonding agent for the reduction and/or prevention of white spot lesions: An in vitro study. *Angle Orthod*, 81, 6, 1014-20.

CAI, F., SHEN, P., MORGAN, M. V. & REYNOLDS, E. C. 2003. Remineralization of enamel subsurface lesions *in situ* by sugar-free lozenges containing casein phosphopeptide-amorphous calcium phosphate. *Aust Dent J*, 48, 240-3.

CAI, Y. 2013. Titanium dioxide photocatalysis in biomaterials applications. *Acta Universitatis Upsaliensis.* Digital Comprehensive Summaries of Uppsala Dissertations from the Faculty of Science and Technology, 1033-58.

CAI, Y., STROMME, M. & WELCH, K. 2013. Photocatalytic antibacterial effects are maintained on resin-based TiO_2 nanocomposites after cessation of UV irradiation. *PLoS One,* 8, 10, 1-8.

CAO, B., WANG, Y., LI, N., LIU, B. & ZHANG, Y. 2013. Preparation of an orthodontic bracket coated with an nitrogen-doped TiO(2-x)N(y) thin film and examination of its antimicrobial performance. *Dent Mater J,* 32, 311-6.

CARATTO, V., BALL, L., SANGUINETI, E., INSORSI, A., FIRPO, I., ALBERTI, S., *et al*. 2017. Antibacterial activity of standard and N-doped titanium dioxide-coated endotracheal tubes: an in vitro study. *Rev Bras Ter Intensiva,* 29, 55-62.

CHA, S., PARK, Y. S. 2014. Plasma in dentistry. *Clin Plasma Med,* 2, 1, 4-10.

CHAMBERS, C., STEWART, S. B., SU, B., JENKINSON, H. F., SANDY, J. R. & IRELAND, A. J. 2017. Silver doped titanium dioxide nanoparticles as antimicrobial additives to dental polymers. *Dent Mater,* 33, e115-e23.

CHAN, D. C., SWIFT, E. J., J. R. & BISHARA, S. E. 1990. In vitro evaluation of a fluoride-releasing orthodontic resin. *J Dent Res,* 69, 1576-9.

CHANG, H. S., WALSH, L. J. & FREER, T. J. 1997. Enamel demineralization during orthodontic treatment. Aetiology and prevention. *Aust Dent J,* 42, 322-7.

CHEN, H., SUN, K., TANG, Z., LAW, R. V., MANSFIELD, J. F. & CLARKSON, B. H. 2006. Synthesis of fluorapatite nanorods and nanowires by direct precipitation from solution. *Cryst Growth Des,* 6, 1504-08.

CLARK, J. R., IRELAND, A. J. & SHERRIFF, M. 2003. An in vivo and ex vivo study to evaluate the use of a glass polyphosphonate cement in orthodontic banding. *Eur J Orthod,* 25, 319-23.

COOK, P. A. & YOUNGSON, C. C. 1989. A fluoride-containing composite resin-an in vitro study of a new material for orthodontic bonding. *Br J Orthod,* 16, 207-12.

CRABB, J. J. & WILSON, H. J. 1971. Use of some adhesives in orthodontics. *Dent Pract Dent Rec,* 22, 111-2.

CRITTENDEN, J. C., SURI, R. P. S., PERRAM, D. L. & HAND, D. W. 1997. Decontamination of water using adsorption and photocatalysis. *Water Research,* 31, 411-418.

CROSS, K. J., HUQ, N. L., PALAMARA, J. E., PERICH, J.W. & REYNOLDS, E. C. 2005. Physicochemical characterization of casein phosphopeptide-amorphous calcium phosphate nanocomplexes. *J Biol Chem*, 280, 15362–69.

DAGHRIR, R., DROGUI, P. & ROBERT, D. 2013. Modified TiO_2 for environmental photocatalytic applications: a review. *Ind Eng Chem Res,* 52, 3581-99.

DAULA, A. U., PFISTER, G. & SCHRAMM, K. W. 2013. Method for toxicity test of titanium dioxide nanoparticles in ciliate protozoan Tetrahymena. *J Environ Sci Health A Tox Hazard Subst Environ Eng*, 48, 11, 1343-48.

DEMITO, C. F., VIVALDI-RODRIGUES, G., RAMOS, A. L. & BOWMAN, S. J. 2004. The efficacy of a fluoride varnish in reducing enamel demineralization adjacent to orthodontic brackets: an in vitro study. *Orthod Craniofac Res,* 7, 205-10.

DEVI, L., NAGARAJ, B. & RAJASHEKHAR, E. 2012. Synergistic effect of Ag deposition and nitrogen doping in TiO_2 for the degradation of phenol under solar irradiation in presence of electron acceptor. *Chem Eng Jour*, 181-82, 259-66.

DOHERTY, U. B., BENSON, P. E. & HIGHAM, S. M. 2002. Fluoride-releasing elastomeric ligatures assessed with the in situ caries model. *Eur J Orthod,* 24, 371-8.

EDGERTON, M., LO, S. E. & SCANNAPIECO, F. A. 1996. Experimental salivary pellicles formed on titanium surfaces mediate adhesion of streptococci. *Int J Oral Maxillofac Implants,* 11, 443-9.

EL-KALLA, I. H. & GARCIA-GODOY, F. 1999. Mechanical properties of compomer restorative materials. *Oper Dent,* 24, 2-8.

ELIADES, T., ELIADES, G. & BRANTLEY, W. A. 1995. Microbial attachment on orthodontic appliances: I. Wettability and early pellicle formation on bracket materials. *Am J Orthod Dentofacial Orthop,* 108, 351-60.

ELLIS, J., ANSTICE, M. & WILSON, A. D. 1991. The glass polyphosphonate cement: a novel glass-ionomer cement based on poly(vinyl phosphonic acid). *Clin Mater,* 7, 341-6.

EMILSON, C. G. 1977. Susceptibility of various microorganisms to chlorhexidine. *Scand J Dent Res,* 85, 255-65.

EPSTEIN, J. B., MCBRIDE, B. C., STEVENSON-MOORE, P., MERILEES, H. & SPINELLI, J. 1991. The efficacy of chlorhexidine gel in reduction of Streptococcus mutans and Lactobacillus species in patients treated with radiation therapy. *Oral Surg Oral Med Oral Pathol,* 71, 172-8.

EVANS, A., LEISHMAN, S. J., WALSH, L. J. & SEOW, W. K. 2015. Inhibitory effects of antiseptic mouthrinses on Streptococcus mutans, Streptococcus sanguinis and Lactobacillus acidophilus. *Aust Dent J,* 60, 247-54.

FAROOQ, I., MOHEET, I., IMRAN, Z. & FAROOQ, U. 2013. A review of novel dental caries preventive material: Casein phosphopeptide–amorphous calcium phosphate (CPP–ACP) complex. *J King Saud Univ Sci*, 4, 47-51.

FARRET, M. M., DE LIMA, E. M., MOTA, E. G., OSHIMA, H. M., BARTH, V. & DE OLIVEIRA, S. D. 2011. Can we add chlorhexidine into glass ionomer cements for band cementation? *Angle Orthod,* 81, 496-502.

FATANI, E. J., ALMUTAIRI, H. H., ALHARBI, A. O., ALNAKHLI, Y. O., DICAKAR, D. D., ALKHERAIF, A. A. *et al*. 2017. In vitro assessment of stainless steel orthodontic brackets coated with titanium oxide mixed Ag for anti-adherent and antibacterial properties against Streptococcus mutans and Porphyromonas gingivalis. *Microb Pathog,* 112, 190-94.

FEATHERSTONE, J. D., GLENA, R., SHARIATI, M. & SHIELDS, C. P. 1990. Dependence of in vitro demineralization of apatite and remineralization of dental enamel on fluoride concentration. *J Dent Res,* 69, 620-5.

FEJERSKOV, O. & KIDD, E. (2008) *Dental caries. The disease and its clinical management*, 2nd edition ed., Copenhagen: Oxford: Blackwell.

FISCHMAN, S. A. & TINANOFF, N. 1994. The effect of acid and fluoride release on the antimicrobial properties of four glass ionomer cements. *Pediatr Dent,* 16**,** 368-70.

FOSTER, J. A., BERZINS, D. W. & BRADLEY, T. G. 2008. Bond strength of an amorphous calcium phosphate-containing orthodontic adhesive. *Angle Orthod,* 78, 339-44.

FUJISHIMA, A. & HONDA, K. 1972. Electrochemical photolysis of water at a semiconductor electrode. *Nature,* 238, 37-38.

GALARRAGA, N. & CROCE, N. 2003. Comparative clinical trials between orthodontic band cements with zinc phosphate and conventional glass ionomer [Estudio cl´ınico comparativo entre el cementado de bandas ortodo´ncicas con fosfato de zinc y con vidrio ionome´rico convencional]. *Latin Am J Orthod Pediatric Dent.*

GEIGER, A. M., GORELICK, L., GWINNETT, A. J. & BENSON, B. J. 1992. Reducing white spot lesions in orthodontic populations with fluoride rinsing. *Am J Orthod Dentofacial Orthop,* 101**,** 403-7.

GIOKA, C., BOURAUEL, C., ZINELIS, S., ELIADES, T., SILIKAS, N. & ELIADES, G. 2004. Titanium orthodontic brackets: structure, composition, hardness and ionic release. *Dent Mater,* 20, 693-700.

GLANS, R., LARSSON, E. & OGAARD, B. 2003. Longitudinal changes in gingival condition in crowded and noncrowded dentitions subjected to fixed orthodontic treatment. *Am J Orthod Dentofacial Orthop,* 124, 679-82.

CONG, Y., ZHANG, J., CHEN, F., ANPO, M. 2007. Synthesis and characterization of nitrogen-doped TiO_2 nanophotocatalyst with high visible light activity. *J Phys Chem C*, 111, 19, 6976-82.

GORELICK, L., GEIGER, A. M. & GWINNETT, A. J. 1982. Incidence of white spot formation after bonding and banding. *Am J Orthod,* 81, 93-8.

GOSH, S. & DAS, A. P. 2015. Modified titanium oxide (TiO_2) nanocomposites and its array of applications: a review. *Toxicol Environ Chem,* 97, 491-514.

GYORGYEY, A., JANOVAK, L., KOPNICZKY, J., TOTH, K. L., PANAYOTOV, I., CUISINIER, F. *et al*. 2016. Investigation of the in vitro photocatalytic antibacterial activity of nanocrystalline TiO_2 and coupled TiO_2/Ag containing copolymer on the surface of medical grade titanium. *J Biomater Appl*, 31, 55-67.

HANNIG, M. 2002. The protective nature of the salivary pellicle. *Int Dent J,* 52, 417-23.

HOSZEK, A. & ERICSON, D. 2008. In vitro fluoride release and the antibacterial effect of glass ionomers containing chlorhexidine gluconate. *Oper Dent,* 33, 696-701.

HOWELLS, D. J. & JONES, P. 1989. In vitro evaluation of a cyanoacrylate bonding agent. *Br J Orthod,* 16, 75-8.

IQBAL, P., PREECE JON, A. & MENDES PAULA, M. 2012. Nanotechnology: The “Top-Down” and “Bottom-Up” Approaches. *Supramolecular Chemistry: From Molecules to Nanomaterials.* John Wiley & Sons, Ltd.

IRELAND, A.J & MCDONALD, F. (2003) *The Orthodontic Patient: Treatment and Biomechanics*, Oxford University Press.

JARVINEN, H., PIENIHAKKINEN, K., HUOVINEN, P. & TENOVUO, J. 1995. Susceptibility of Streptococcus mutans and Streptococcus sobrinus to antimicrobial agents after short-term oral chlorhexidine treatments. *Eur J Oral Sci,* 103, 32-5.

JEON, H. S., CHOI, C. H., KANG, S. M., KWON, H. K. & KIM, B. I. 2015. Chlorhexidine-releasing orthodontic elastomerics. *Dent Mater J,* 34, 321-6.

KAMARUDIN, Y. 2017. In-vitro study of chlorohexidine hexametaphosphate nanoparticles to produce a sustained chlorhexidine release environment to reduce white spot lesions in orthodontic patients. Master's thesis, University of Bristol, Bristol.

KANAPARTHY, R. & KANAPARTHY, A. 2011. The changing face of dentistry: nanotechnology. *Int J Nanomedicine,* 6, 2799-804.

KARABELA, M., SIDERIDOU, I. 2011. Synthesis and study of properties of dental resin composites with different nanosilica particles size. *Dent Mat,* 27, 825-35.

KAUTSKY, M. B. & FEATHERSTONE, J. D. 1993. Effect of salivary components on dissolution rates of carbonated apatites. *Caries Res,* 27, 373-7.

KHOROUSHI, M. & KESHANI, F. 2013. A review of glass-ionomers: From conventional glass-ionomer to bioactive glass-ionomer. *Dent Res J,* 10, 411-20.

KIM, T. H., GO, G. M., CHO, H. B., SONG, Y., LEE, C. G. & CHOA, Y. H. 2018. A novel synthetic method for N doped TiO_2 nanoparticles through plasma-assisted electrolysis and photocatalytic activity in the visible region. *Front Chem*, 6, 456.

KLOCKE, A., TADIC, D., KAHL-NIEKE, B. & EPPLE, M. 2003. An optimized synthetic substrate for orthodontic bond strength testing. *Dent Mater,* 19, 773-8.

KUMAR, M. & KUMARI, S. 2016. Resin-modified glass ionomer cement and its use in orthodontics - concept old is gold: view point. *Int J Dent Med Spec Renu Publishers*.

KVAM, E., BROCH, J. & NISSEN-MEYER, I. H. 1983. Comparison between a zinc phosphate cement and a glass ionomer cement for cementation of orthodontic bands. *Eur J Orthod,* 5, 307-13.

LE, P. T., WEINSTEIN, M., BORISLOW, A. J. & BRAITMAN, L. E. 2003. Bond failure and decalcification: A comparison of a cyanoacrylate and a composite resin bonding system in vivo. *Am J Orthod Dentofacial Orthop,* 123, 624-7.

LEE, S. J., KHO, H. S., LEE, S. W. & YANG, W. S. 2001. Experimental salivary pellicles on the surface of orthodontic materials. *Am J Orthod Dentofacial Orthop,* 119, 59-66.

LEE, S. M., FREER, T. J. & BASFORD, K. E. 1986. Microleakage at the etched enamel-resin interface with bonded orthodontic brackets. *Aust Orthod J,* 9, 270-5.

LEE, S. Y., KANG, D., JEONG, S., DO, H. T. & KIM, J. H. 2020. Photocatalytic degradation of Rhodamine B dye by TiO_2 and gold nanoparticles supported on a floating porous polydimethylsiloxane sponge under ultraviolet and visible light irradiation. *ACS Omega,* 5, 8, 4233-41.

LEGEROS, R. Z. & TUNG, M. S. 1983. Chemical stability of carbonate- and fluoride-containing apatites. *Caries Res,* 17**,** 419-29.

LIN, J., ZHU, J., GU, X., WEN, W., LI, Q., FISCHER-BRANDIES, H., *et al*. 2011. Effects of incorporation of nano-fluorapatite or nano-fluorohydroxyapatite on a resin-modified glass ionomer cement. *Acta Biomater,* 7, 1346-53.

LIVRAGHI, S., ELGHNIJI, K., CZOSKA, A. M., PAGANINI, M. C., GIAMELLO, E. & KSIBI, M. 2009. Nitrogen-doped and nitrogen–fluorine-codoped titanium dioxide. Nature and concentration of the photoactive species and their role in determining the photocatalytic activity under visible light. *J Photochem Photobiol,* 205, 93-97.

LU, Y. M., LIU, C. K. & HUANG, C. M. 2007. The visible photocatalyst properties of Nitrogen-doped TiO_2 thin film. *ECS Transactions,* 2, 101-107.

MAIJER, R. & SMITH, D. C. 1982. Corrosion of orthodontic bracket bases. *Am J Orthod,* 81, 43-8.

MANTON, D. J., WALKER, G. D., CAI, F., COCHRANE, N. J., SHEN, P. & REYNOLDS, E. C. 2008. Remineralization of enamel subsurface lesions in situ by the use of three commercially available sugar-free gums. *Int J Paediatr Dent,* 18, 284-90.

MARGOLIS, H. C. & MORENO, E. C. 1990. Physicochemical perspectives on the cariostatic mechanisms of systemic and topical fluorides. *J Dent Res,* 69, 606-13.

MARINHO, V. C., CHONG, L. Y., WORTHINGTON, H. V. & WALSH, T. 2016. Fluoride mouthrinses for preventing dental caries in children and adolescents. *Cochrane Database Syst Rev,* 7, CD002284.

MARSH, P. D. 1993. Antimicrobial strategies in the prevention of dental caries. *Caries Res,* 1, 72-6.

MARTINEZ, A. W. & CHAIKOF, E. L. 2011. Microfabrication and nanotechnology in stent design. *Wiley Interdiscip Rev Nanomed Nanobiotechnol,* 3, 256-68.

MATTHIAS, H., CHRISTIAN, H., AHMED, W. & HARTSFIELD, J. K. 2013. Chapter 8 - nanobiomaterials in preventive dentistry A2 - Subramani, Karthikeyan. *Nanobiomaterials in Clinical Dentistry.* William Andrew Publishing.

MATTHIJS, S. & ADRIAENS, P. A. 2002. Chlorhexidine varnishes: a review. *J Clin Periodontol,* 29, 1-8.

MATTOUSCH, T. J., VAN DER VEEN, M. H. & ZENTNER, A. 2007. Caries lesions after orthodontic treatment followed by quantitative light-induced fluorescence: a 2-year follow-up. *Eur J Orthod,* 29, 294-8.

MEKPRASART, W., KHUMTONG, T., RATTANARAK, J., TECHITDHEERA, W. & PECHARAPA, W. 2013. Effect of nitrogen doping on optical and photocatalytic properties of TiO_2 thin film prepared by spin coating process. *Energy Procedia,* 34, 746-50.

MELLANBY, M. 1930. Diet and the teeth: An experimental study. Part II. A diet and dental structure in mammals and other than the dog. *Medical research Council. London: His Majesty's Stationary office Special Report Series*, 153, 162-278.

MIHARDJANTI, M., ISMAH, N. & PURWANEGARA, M. K. 2017. Nickel and chromium ion release from stainless steel bracket on immersion various types of mouthwashes. *J Phys Conf Ser,* 884, 012107.

MILLETT, D. T., MCCLUSKEY, L. A., MCAULEY, F., CREANOR, S. L., NEWELL, J. & LOVE, J. 2000. A comparative clinical trial of a compomer and a resin adhesive for orthodontic bonding. *Angle Orthod,* 70, 233-40.

MIZRAHI, E. 1982. Enamel demineralization following orthodontic treatment. *Am J Orthod,* 82, 62-7.

MOHAMED HAMOUDA, I. 2012. Current perspectives of nanoparticles in medical and dental biomaterials. *J Biomed Res,* 26, 143-51.

MOHN, D., ZEHNDER, M., IMFELD, T. & STARK, W. J. 2010. Radio-opaque nanosized bioactive glass for potential root canal application: evaluation of radiopacity, bioactivity and alkaline capacity. *Int Endod J,* 43, 210-7.

MONTEIRO, R., MIRANDA, S., VILAR, V., PASTRANA-MARTINEZ, L., TAVARES, P., BOAVENTURA, R., *et al*. 2014. N-modified TiO_2 photocatalytic activity towards diphenhydramine degradation and Escherichia coli inactivation in aqueous solutions. *Applied Cat B: Env*, 162, 66-74.

MOOSAVI, M. A., SHARIFI, M., GHAFARY, S. M., MOHAMMADALIPOUR, Z., KHATAEE, A., RAHMATI, M., *et al*. 2016. Photodynamic N-TiO. *Sci Rep,* 6, 34413.

MORGAN, M. V., ADAMS, G. G., BAILEY, D. L., TSAO, C. E., FISCHMAN, S. L. & REYNOLDS, E. C. 2008. The anticariogenic effect of sugar-free gum containing CPP-ACP nanocomplexes on approximal caries determined using digital bitewing radiography. *Caries Res*, 42, 171-84.

MOTA, S. M., ENOKI, C., ITO, I. Y., ELIAS, A. M. & MATSUMOTO, M. A. 2008. Streptococcus mutans counts in plaque adjacent to orthodontic brackets bonded with resin-modified glass ionomer cement or resin-based composite. *Braz Oral Res,* 22, 55-60.

MROWETZ, M., BACERSKI, W., COLUSSI, A.J. & HOFFMANN, M. R. 2004. Oxidative power of nitrogen-doped TiO_2 photocatalysts under visible illumination. *J Phys Chem B,* 108, 45, 17269-73.

MUELLER, H. J. & BAPNA, M. S. 1993. Microstructural enhancement of dental composite and ceramic materials by plasma etching. *Cells and Materials*, 3, 37-43.

MUGGLI, D. S. & DING, L. 2001a. Photocatalytic performance of sulfated TiO 2 and degussa P-25 TiO 2 during oxidation of organics. *Appl Catal B,* 32, 181-194.

MURPH, S. E., COOPERSMITH, K. J. & LARSEN, G. K. 2017. Anisotropic and shape-selective nanomaterials, nanostructure science and technology. *Nanoscale Materials: Fundamentals and Emergent Properties.* Springer International Publishing.

NASIRIAN, M., LIN, Y. P., BUSTILLO-LECOMPTE, C. F. & MEHRVAR, M. 2018. Enhancement of photocatalytic activity of titanium dioxide using non-metal doping methods under visible light: a review. *Int J Environ Sci Technol*, 15, 2009-32.

NEWMAN, G. V. 1969. Adhesion and orthodontic plastic attachments. *Am J Orthod,* 56, 573-88.

OGAARD, B., LARSSON, E., GLANS, R., HENRIKSSON, T. & BIRKHED, D. 1997. Antimicrobial effect of a chlorhexidine-thymol varnish (Cervitec) in orthodontic patients. A prospective, randomized clinical trial. *J Orofac Orthop,* 58, 206-13.

OGAARD, B., LARSSON, E., HENRIKSSON, T., BIRKHED, D. & BISHARA, S. E. 2001. Effects of combined application of antimicrobial and fluoride varnishes in orthodontic patients. *Am J Orthod*, 120, 1, 28-35.

OHNO, T., SARUKAWA, K., TOKIEDA, K. & MATSUMURA, M. 2001. Morphology of a TiO 2 Photocatalyst (Degussa, P-25) Consisting of Anatase and Rutile Crystalline Phases. *J Catal,* 203**,** 82-86.

OLYMPIO, K. P., BARDAL, P. A., DE, M. B. J. R. & BUZALAF, M. A. 2006. Effectiveness of a chlorhexidine dentifrice in orthodontic patients: a randomized-controlled trial. *J Clin Periodontol,* 33, 421-6.

PAULOS, R. S., SEINO, P. Y., FUKUSHIMA, K. A., MARQUES, M. M., DE ALMEIDA, F. C. S., RAMALHO, K. M.*, et al*. 2017. Effect of Nd:YAG and CO_2 laser irradiation on prevention of enamel demineralization in orthodontics: *in vitro* study. *Photomed Laser Surg,* 35, 282-86.

RATTANAKAM, R. & SUPOTHINA, S. 2009. Visible-light-sensitive N-doped TiO_2 photocatalysts prepared by a mechanochemical method: effect of a nitrogen source. *Res Chem Intermed,* 35, 263-269.

PAWAR, M., SENDOGDULAR, S. T. & GOUMA, P. 2018. A brief overview of TiO_2 photocatalyst for organic dye remediation: case study of reaction mechanisms involved in Ce-TiO_2 photocatalysts system. *J Nanomater*, 1-13.

PERAL, J., DOMÈNECH, X. & OLLIS, D. F. 1997. Heterogeneous photocatalysis for purification, decontamination and deodorization of air. *J Chem Technol Biotechnol,* 70, 117-40.

PICHAT, P. 1986. Adsorption and Desorption Processes in Photocatalysis. *Homogeneous and Heterogeneous Photocatalysis,* 174, 533-554.

PITHON, M. M., DOS SANTOS, M. J., ANDRADE, C. S. S., LEAO FILHO, J. C. B., BRAZ, A. K. S., DE ARAUJO, R. E., *et al*. 2015. Effectiveness of varnish with CPP–ACP in prevention of caries lesions around orthodontic brackets: an OCT evaluation. *Eur J Orthod*, 37, 2, 177-82.

POLAND, C. A., DUFFIN, R., KINLOCH, I., MAYNARD, A., WALLACE, W. A., SEATON, A., *et al*. 2008. Carbon nanotubes introduced into the abdominal cavity of mice show asbestos-like pathogenicity in a pilot study. *Nat Nanotechnol,* 3, 423-8.

PUIG SILLA, M., MONTIEL COMPANY, J. M. & ALMERICH SILLA, J. M. 2008. Use of chlorhexidine varnishes in preventing and treating periodontal disease. A review of the literature. *Med Oral Patol Oral Cir Bucal,* 13, E257-60.

RAHILLY, G. & PRICE, N. 2003. Nickel allergy and orthodontics. *J Orthod,* 30, 171-4.

RANJAN, R, KRISHNAMRAJU, P. V., SHANKAR, T. 2017. Nonthermal plasma in dentistry: an update. *J Int Soc Prev Community Dent*, 7, 3, 71-75.

REDLICH, M., KATZ, A., RAPOPORT, L., WAGNER, H. D., FELDMAN, Y. & TENNE, R. 2008. Improved orthodontic stainless steel wires coated with inorganic fullerene-like nanoparticles of WS(2) impregnated in electroless nickel-phosphorous film. *Dent Mater,* 24, 1640-6.

REYNOLDS, E. C. 1998. Anticariogenic complexes of amorphous calcium phosphate stabilized by casein phosphopeptides: a review. *Spec Care Dentist,* 18, 8-16.

REYNOLDS, E. C., CAI, F., SHEN, P. & WALKER, G. D. 2003. Retention in plaque and remineralization of enamel lesions by various forms of calcium in a mouthrinse or sugar-free chewing gum. *J Dent Res*, 82, 206-11.

REYNOLDS, R. 2016. A review of direct orthodontic bonding. *British J Orthodontics,* 2, 171-178.

RIBEIRO, J. & ERICSON, D. 1991. In vitro antibacterial effect of chlorhexidine added to glass-ionomer cements. *Scand J Dent Res,* 99, 533-40.

RIEHEMANN, K., SCHNEIDER, S. W., LUGER, T. A., GODIN, B., FERRARI, M. & FUCHS, H. 2009. Nanomedicine-challenge and perspectives. *Angew Chem Int Ed Engl,* 48, 872-97.

ROCK, W. P. & ABDULLAH, M. S. 1997. Shear bond strengths produced by composite and compomer light cured orthodontic adhesives. *J Dent,* 25, 243-9.

ROSIN-GRGET, K., PEROS, K., SUTEJ, I. & BASIC, K. 2013. The cariostatic mechanisms of fluoride. *Acta Med Acad,* 42, 179-88.

RUPP, F., HAUPT, M., KLOSTERMANN, H., KIM, H. S., EICHLER, M., PEETSCH, A., *et al*. 2010. Multifunctional nature of UV-irradiated nanocrystalline anatase thin films for biomedical applications. *Acta Biomater,* 6, 4566-77.

RUSSELL, J. S. 2005. Aesthetic orthodontic brackets. *J Orthod,* 32, 146-63.

SADR HAGHIGHI, H., SKANDARINEJAD, M. & ABDOLLAHI, A. A. 2013. Laser application in prevention of demineralization in orthodontic Treatment. *J Lasers Med Sci,* 4, 107-10.

SAFENANO, I. 2017. *Vision, Mision and Values* [Online]. Available: safenano.org/about/mission/ [Accessed 23rd December 2017].

SARI, E. & BIRINCI, I. 2007. Microbiological evaluation of 0.2% chlorhexidine gluconate mouth rinse in orthodontic patients. *Angle Orthod,* 77, 881-4.

SHAHAL, Y., STEINBERG, D., HIRSCHFELD, Z., BRONSHTEYN, M. & KOPOLOVIC, K. 1998. In vitro bacterial adherence onto pellicle-coated aesthetic restorative materials. *J Oral Rehabil,* 25, 52-8.

SHEN, P., CAI, F., NOWICKI, A., VINCENT, J. & REYNOLDS, E. C. 2001. Remineralization of enamel subsurface lesions by sugar-free chewing gum containing casein phosphopeptide-amorphous calcium phosphate. *J Dent Res,* 80, 2066-70.

SINGH, C., DUA, V., VYAS, M. & VERMA, S. 2013. Evaluation of the antimicrobial and physical properties of an orthodontic photo-activated adhesive modified with an antiplaque agent: an in vitro study. *Indian J Dent Res,* 24, 694-700.

SMITH, D. C. 1998. Development of glass-ionomer cement systems. *Biomaterials,* 19, 467-78.

STARR, CECIE. 2005. Biology: Concepts and Applications (6th Ed.). Boston, United States, Thomson Brooks/Cole, 94.

SUDJALIM, T. R., WOODS, M. G., MANTON, D. J. & REYNOLDS, E. C. 2007. Prevention of demineralization around orthodontic brackets *in vitro*. *Am J Orthod Dentofacial Orthop*, 131, 705, e1-9.

SUKONTAPATIPARK, W., EL-AGROUDI, M. A., SELLISETH, N. J., THUNOLD, K. & SELVIG, K. A. 2001. Bacterial colonization associated with fixed orthodontic appliances. A scanning electron microscopy study. *Eur J Orthod,* 23, 475-84.

SUMMITT, J. B., ROBBINS, J.W. & SCHWARTZ, R. S. 2006. Fundamentals of Operative Dentistry: A Contemporary Approach, 3rd Edition ed., *Quintessence Publishing Company*, Michigan.

TANG, X., SENSAT, M. L. & STOLTENBERG, J. L. 2016. The antimicrobial effect of chlorhexidine varnish on mutans streptococci in patients with fixed orthodontic appliances: a systematic review of clinical efficacy. [Review]. *Int J Dent Hyg,* 14, 53-61.

TAUC, J. 1968. Optical properties and electronic structure of amorphous Ge and Si. *Mater Res Bull,* 3, 37–46.

TEN CATE, J. M. & FEATHERSTONE, J. D. B. 1996. Physiochemical aspects of fluoride-enamel interactions. *In:* FEJERSKOV, O., EKSTRAND, J. & BURT, B. A. (eds.) *Fluoride in dentistry.* 2nd Edition ed. Copenhagen.

TWETMAN, S., HALLGREN, A. & PETERSSON, L. G. 1995. Effect of an antibacterial varnish on mutans streptococci in plaque from enamel adjacent to orthodontic appliances. *Caries Res,* 29, 188-91.

UYSAL, T., AMASYALI, M., OZCAN, S., KOYUTURK, A. E., AKYOL, M. & SAGDIC, D. 2010. In vivo effects of amorphous calcium phosphate-containing orthodontic composite on enamel demineralization around orthodontic brackets. *Aust Dent J,* 55, 285-91.

VAN DER LINDEN, R. P. & DERMAUT, L. R. 1998. White spot formation under orthodontic bands cemented with glass ionomer with or without Fluor Protector. *Eur J Orthod,* 20, 219-24.

VAN DIJKEN, J. W. V. 1987. Conventional, microfilled and hybrid composite resins: laboratory and clinical evaluations. *Umeå University odontological dissertations*, 59.

VAN GASTEL, J., QUIRYNEN, M., TEUGHELS, W., PAUWELS, M., COUCKE, W. & CARELS, C. 2009. Microbial adhesion on different bracket types in vitro. *Angle Orthod,* 79, 915-21.

VON FRAUNHOFER, J. A., ALLEN, D. J. & ORBELL, G. M. 1993. Laser etching of enamel for direct bonding. *Angle Orthod,* 63, 73-6.

WHITE, R. J. 2001. An historical overview on the use of silver in modern wound management. *British J Nursing, 10, S3-8.*

WALSH L. J. 2009. The current status of tooth cremes for enamel remineralisation. *Dental Inc*, 2, 38-2.

WILTSHIRE, W. A. 1996. Determination of fluoride from fluoride-releasing elastomeric ligature ties. *Am J Orthod Dentofacial Orthop,* 110, 383-7.

WU, D., LONG, M., CAI, W., CHEN, C. & WU, Y. 2010. Low temperature hydrothermal synthesis of N-doped TiO_2 photocatalyst with high visible-light activity. *Alloy Cmpd,* 502, 2, 289-94.

WU, J., WEIR, M. D., MELO, M. A. & XU, H. H. 2015. Development of novel self-healing and antibacterial dental composite containing calcium phosphate nanoparticles. *J Dent,* 43, 317-26.

XIA, T., LI, N. & NEL, A. E. 2009. Potential health impact of nanoparticles. *Annu Rev Public Health,* 30, 137-50.

XIONG, L. B., LI, J. L., YANG, B. & YU, Y. 2012. Ti3+ in the Surface of Titanium Dioxide: Generation, Properties and Photocatalytic Application. *Jour Nano*, 1-13.

XU, Q., ZHANG, W., DONG, C., SREEPRASAD, T. S. & XIA, Z. 2016. Biomimetic self-cleaning surfaces: synthesis, mechanism and applications. *J R Soc Interface,* 122.

YANG, H. & YANG, J. 2018. Photocatalytic degradation of rhodamine B catalyzed by TiO_2 films on a capillary column. *RCS Adv*, 8, 11921-29.

YIN, S., SATO, T. & ZHANG, Q. 2003. Preparation of visible light-activated titania photocatalyst by mechanochemical method. *Chemistry Lett,* 32, 4, 358-59.

YING, D., CHUAH, G. K. & HSU, C. Y. 2004. Effect of Er:YAG laser and organic matrix on porosity changes in human enamel. *J Dent,* 32, 41-6.

YOSHIDA, T., NIIMI, S., YAMAMOTO, M., NOMOTO, T. & YAGI, S. 2015. Effective nitrogen doping into TiO_2 (N-TiO_2) for visible light response photocatalysis. *J Colloid Interface Sci,* 447, 278-81.

ZALESKA, A. 2008. Doped TiO_2: a review. *Recent Patents on Engineering*, 2, 157-64.